Supporting Information

for

Modified Nucleoside Triphosphates Exist in Mammals

Han-Peng Jiang,† Jun Xiong,† Fei-Long Liu, Cheng-Jie Ma, Xing-Lin Tang, Bi-Feng Yuan,*

Yu-Qi Feng

Key Laboratory of Analytical Chemistry for Biology and Medicine (Ministry of Education), Department of Chemistry, Wuhan University, Wuhan 430072, China.

† These authors contributed equally to this work.

* To whom correspondence should be addressed. Tel. +86-27-68755595; fax. +86-27-68755595. E-mail address: bfyuan@whu.edu.cn

Method Validation

To construct the calibration curves, a mixture of NTP standards at concentrations between 10 and 2500 fmol/μL and fixed amounts of isotope internal standards ($^{13}C_{10}$,$^{15}N_5$-ATP for the ribonucleotides and $^{13}C_{10}$,$^{15}N_5$-dATP for the 2'-deoxyribonucleotides, 20 fmol/μL for each) was prepared. The calibration curves of NTPs were constructed in cellular extraction matrix. A cellular extract without adding the mixture of NTP standards was used as the background. The mixture was labeled by 8-DMQ and then analyzed by LC-ESI-MS/MS. So the calibration curves were generated by plotting the peak area ratios (analytes/IS) against the NTPs concentrations after deduction of background with triplicate measurements. The results showed that good linearities were obtained with the coefficient of determination (R^2) being great than 0.9909 (Table S5 in Supporting Information). The limits of detection (LODs) were much better than the LODs obtained by the previously established methods (Table S3 in Supporting Information).

In addition, the precision and accuracy of established method were evaluated by comparing the measured contents of NTPs standards to the theoretical contents of NTPs. The intra- and inter-day relative standard deviations (RSDs) were calculated with different amounts of NTPs standards spiked in cell extraction mixture. Three measurements over a day gave the intra-day RSDs, and the inter-day RSDs were determined by measuring samples for three consecutive days. The results showed that the intra- and inter-day RSDs for NTPs were less than 14.9%, and relative errors (REs) were less than 14.0% (Table S6 in Supporting Information), indicating good precision and accuracy were achieved. Taken together, the results demonstrated that the developed method was reliable for the quantification of NTPs.

Evaluation of the stable isotope labeling efficiency by D_3-Met

Human 293T cells were cultured in the methionine-free DMEM-KO medium with the added stable isotope labeled methionine, D_3-Met, to metabolically label the DNA and RNA

with CD_3 group. Cells were collected after 48 h culturing and genomic DNA and total RNA were then extracted and enzymatically digested into nucleosides to quantify the stable isotope forms of nucleosides (Figure S9 in Supporting Information). The results showed that 7 kinds of nucleosides and the corresponding CD_3-labeled nucleosides, including CD_3-m^1A, CD_3-m^6A, CD_3-Am, CD_3-Gm, CD_3-m^1G, CD_3-5-mC and CD_3-5-mdC, were clearly detected. With the measured contents of the stable isotope as well as the non-isotope forms of these methylated nucleosides, the stable isotope labeling efficiencies were calculated to be between 78% and 97% (Figure S12 in Supporting Information), indicating good stable isotope labeling of DNA and RNA.

Table S1. Nucleosides triphosphate standards.

	Abbreviation	Company	Catalog No.	$[M+H]^+$	Product ion
N^4-Methyl-2'-deoxycytidine-5'-triphosphate	N^4-medCTP	Trilink	N-2057	482.0125	126.0662
N^6-Methyl-2'-deoxyadenosine-5'-triphosphate	N^6-medATP	Trilink	N-2025	506.0238	150.0774
5-Methyl-2'-deoxycytidine-5'-triphosphate	5-medCTP	Trilink	N-2026	482.0125	126.0662
5-Hydroxymethyl-2'-deoxycytidine-5'-triphosphate	5-hmdCTP	Trilink	N-2060	498.0074	142.0611
5-Formyl-2'-deoxycytidine-5'-triphosphate	5-fodCTP	Trilink	N-2064	495.9918	140.0455
5-Carboxy-2'-deoxycytidine-5'-triphosphate	5-cadCTP	Trilink	N-2063	514.0024	156.0404
N^1-Methylguanosine-5'-triphosphate	N^1-meGTP	Trilink	N-1039	538.0186	166.0723
N^1-Methyladenosine-5'-triphosphate	N^1-meATP	Trilink	N-1042	522.0187	150.0774
N^6-Methyladenosine-5'-triphosphate	N^6-meATP	Trilink	N-1013	522.0187	150.0774
O^6-Methylguanosine-5'-triphosphate	O^6-meGTP	Trilink	N-1031	540.0292	168.0880
2'-*O*-Methylpseudouridine-5'-triphosphate	2'-*O*-meYTP	Trilink	N-1041	498.9915	113.0346
2'-*O*-Methyladenosine-5'-triphosphate	2'-*O*-meATP	Trilink	N-1015	522.0187	136.0618
2'-*O*-Methylguanosine-5'-triphosphate	2'-*O*-meGTP	Trilink	N-1017	538.0186	152.0576
2'-*O*-Methylcytidine-5'-triphosphate	2'-*O*-meCTP	Trilink	N-1016	498.0074	112.0505
2'-*O*-Methyluridine-5'-triphosphate	2'-*O*-meUTP	Trilink	N-1018	498.9915	113.0346
2'-*O*-Methylinosine-5'-triphosphate	2'-*O*-meITP	Trilink	N-1021	541.0113	169.0720
2-Thiouridine-5'-triphosphate	2-S-UTP	Trilink	N-1032	500.9530	129.0117
5-Methyluridine-5'-triphosphate	5-meUTP	Trilink	N-1024	498.9915	127.0502
5-Carboxymethylesteruridine-5'-triphosphate	5-caesUTP	Trilink	N-1096	542.9812	171.0400
5-Methylcytidine-5'-triphosphate	5-meCTP	Trilink	N-1014	498.0074	126.0662
5-Hydroxymethylcytidine-5'-triphosphate	5-hmCTP	Trilink	N-1087	514.0024	142.0611
5-Formylcytidine-5'-triphosphate	5-foCTP	Trilink	N-1085	511.9867	140.0455
*N*7-methylguanosine-5'-triphosphate	7-meGTP	Sigma-Aldrich	M6133	539.0209	166.0723
Inosine-5'-triphosphate	ITP	Trilink	N-1020	508.9870	137.0458
Xanthosine-5'-triphosphate	XTP	Trilink	N-1023	524.9820	153.0407
Pseuouridine-5'-triphosphate	YTP	Trilink	N-1019	498.9915	113.0346
2'-deoxyadenosine-5'-triphosphate	dATP	Sigma-Aldrich	30927	492.0081	136.0618
2'-deoxycytidine-5'-triphosphate	dCTP	Sigma-Aldrich	D4635	467.9969	112.0505
2'-deoxyguanosine-5'-triphosphate	dGTP	Sigma-Aldrich	11051466001	508.0030	152.0576
2'-deoxythymidine-5'-triphosphate	TTP	Sigma-Aldrich	T0251	482.9965	127.0502
Adenosine-5'-triphosphate	ATP	Sigma-Aldrich	A26209	508.0030	136.0618
Cytidine-5'-triphosphate	CTP	Sigma-Aldrich	C1506	483.9918	112.0505
Guanosine-5'-triphosphate	GTP	Sigma-Aldrich	G8877	523.9979	152.0576
Uridine-5'-triphosphate	UTP	Sigma-Aldrich	94370	484.9758	113.0346

Table S2. The MRM parameters for the analysis of 8-MQ-NTPs.

Analytes	Scan mode	Precursor ion (*m/z*)	Product ion (*m/z*)	Collision energy (eV)
8-MQ-N^4-medCTP	+	623.1	126.1	45
8-MQ-N^6-medATP	+	647.1	150.1	45
8-MQ-5-medCTP	+	623.1	126.1	45
8-MQ-5-hmdCTP	+	639.1	142.1	45
8-MQ-5-fodCTP	+	637.1	140.1	47
8-MQ-5-cadCTP	+	653.1	156.1	47
8-MQ-N^1-meGTP	+	679.1	166.1	45
8-MQ-N^1-meATP	+	663.1	150.1	45
8-MQ-N^6-meATP	+	663.1	150.1	45
8-MQ-O^6-meGTP	+	679.1	168.1	47
8-MQ-2'-*O*-meYTP	+	640.1	113.1	47
8-MQ-2'-*O*-meATP	+	663.1	136.1	47
8-MQ-2'-*O*-meGTP	+	679.1	152.1	47
8-MQ-2'-*O*-meCTP	+	639.1	112.1	47
8-MQ-2'-*O*-meUTP	+	640.1	113.1	47
8-MQ-2'-*O*-meITP	+	664.1	169.1	47
8-MQ-2-*S*-UTP	+	642.1	129.1	47
8-MQ-5-meUTP	+	640.1	127.1	47
8-MQ-5-caesUTP	+	684.1	171.2	47
8-MQ-5-meCTP	+	639.1	126.1	45
8-MQ-5-hmCTP	+	655.1	142.1	45
8-MQ-5-foCTP	+	653.1	140.1	47
8-MQ-7-meGTP	+	679.1	166.1	47
8-MQ-ITP	+	650.1	137.1	47
8-MQ-XTP	+	666.1	153.1	47
8-MQ-YTP	+	626.1	113.1	47
8-MQ-dATP	+	633.1	136.1	47
8-MQ-dCTP	+	609.1	112.1	47
8-MQ-dGTP	+	649.1	152.1	47
8-MQ-TTP	+	624.1	127.1	47
8-MQ-ATP	+	649.1	136.1	47
8-MQ-CTP	+	625.1	112.1	47
8-MQ-GTP	+	665.1	152.1	47
8-MQ-UTP	+	626.1	113.1	47

Table S3. Comparison of our developed chemical labeling coupled with LC-ESI-MS/MS method with other methods.

Detection Methods	Samples analyzed	Analytes	LOD (pmol)	References	Year
CE-UV	Standard sample	ATP, GTP, UTP	2200 - 4200	1	1996
HPLC-electrochemical detection	*E. coli* cells	dATP, dCTP, dGTP, TTP, 8-oxodGTP	6	2	2002
CE-UV	CHO cells	ATP, CTP, GTP, UTP	12 - 85	3	2008
Ion-pair HPLC-MS/MS	*S. cerevisiae, Penicillium chrysogenum* and *Escherichia coli*	ATP, CTP, GTP, UTP, ITP	0.06 - 0.12	4	2009
Ion-pair HPLC-MS	Cauliflower and beer	ATP, CTP, GTP, UTP, TTP	3.0 - 3.2	5	2010
Ion-pair UPLC-MS/MS coupled with dispersive solid phase extraction	*Lactococcus lactis*	8 canonical NTPs	2.2 - 15.8	6	2013
HPLC-UV	Royal jelly	ATP	1.9	7	2015
HPLC-UV	Seaweeds	ATP	19	8	2016
HPLC-MS/MS	Human cancer cell	NTP analogues	0.5	9	2017
HPLC-MS/MS	Sturgeon spermatozoa	ATP	1.9	10	2017
Chemical labeling coupled with LC-ESI-MS/MS	Multiple mammalian cells and human tissues	20 NTPs	0.0004 - 0.003	Current study	2017

Table S4. Contents of the detected NTPs in cultured cells.

Modified NTPs	Contents of NTPs (fmol/mg protein)		
	293T cells	HeLa cells	Jurkat-T cells
5-medCTP	2.4 ± 0.13	2.0 ± 0.11	2.9 ± 0.13
5-hmdCTP	3.2 ± 0.31	2.7 ± 0.22	3.3 ± 0.32
N^1-meATP	2.2 ± 0.07	2.5 ± 0.23	2.9 ± 0.10
N^6-meATP	2.3 ± 0.16	2.2 ± 0.11	3.0 ± 0.10
2'-*O*-meATP	2.9 ± 0.14	2.5 ± 0.21	2.4 ± 0.11
2'-*O*-meGTP	1.7 ± 0.12	1.5 ± 0.12	2.0 ± 0.10
2-*S*-UTP	13.2 ± 0.74	5.0 ± 0.10	2.5 ± 0.21
5-meCTP	5.2 ± 0.51	4.1 ± 0.30	4.8 ± 0.20
5-hmCTP	1.9 ± 0.09	1.0 ± 0.04	1.3 ± 0.11
7-meGTP	7.5 ± 0.64	6.1 ± 0.32	8.4 ± 0.94
ITP	12.8 ± 1.21	6.9 ± 0.73	11.2 ± 0.73
XTP	2.9 ± 0.11	2.3 ± 0.21	3.5 ± 0.21

*n.d., not detected.

Table S5. Linearities, LODs and LOQs of NTPs with 8-DMQ labeling followed by LC-ESI-MS/MS analysis.

Analytes	Linear range (fmol/μL)	Calibration curve data			LOD (fmol)	LOQ (fmol)
		Slope	Intercept	R^2 value		
8-MQ-5-medCTP	10-2500	0.0086	-0.2922	0.9998	1.0	3.2
8-MQ-5-hmdCTP		0.0092	-0.0257	0.9987	1.9	6.2
8-MQ-N^1-meATP		0.0096	-0.3273	0.9987	0.9	3.0
8-MQ-N^6-meATP		0.0542	-2.2522	0.9927	0.4	1.3
8-MQ-2'-*O*-meATP		0.0473	-2.2330	0.9903	0.4	1.3
8-MQ-2'-*O*-meGTP		0.0217	-0.6158	0.9958	0.7	2.1
8-MQ-2-*S*-UTP		0.0087	-0.2838	0.9933	1.2	3.2
8-MQ-5-meCTP		0.0049	-0.2574	0.9929	1.9	6.3
8-MQ-5-hmCTP		0.0038	-0.1844	0.9936	2.5	8.2
8-MQ-7-meGTP		0.0013	-0.1525	0.9913	2.9	9.7
8-MQ-ITP		0.0103	-0.2949	0.9963	0.8	2.5
8-MQ-XTP		0.0022	-0.0928	0.9974	2.0	6.5
8-MQ-dATP		0.0889	-0.7845	0.9952	0.4	1.3
8-MQ-dCTP		0.0173	-0.6009	0.9987	0.6	2.1
8-MQ-dGTP		0.0155	-0.0524	0.9993	1.1	3.2
8-MQ-TTP		0.0337	0.0138	0.9974	0.5	1.5
8-MQ-ATP		0.0966	-5.4890	0.9909	0.6	2.1
8-MQ-CTP		0.0073	-0.3217	0.9964	1.3	4.2
8-MQ-GTP		0.0230	-0.6791	0.9987	0.6	1.9
8-MQ-UTP		0.0004	-0.0244	0.9974	2.9	9.7

Table S6. Accuracy and precision for the detection of modified NTPs by 8-DMQ labeling coupled with LC-ESI-MS/MS analysis.

Analytes	QCs	Theoretical value (fmol/μL)	Measured value (fmol/μL)	Relative error (%)	Intra-day RSD%, n=3	Inter-day RSD%, n=3
	Low	20	19	-5.0	9.5	8.7
8-MQ-5-medCTP	Medium	100	88	-12.0	7.1	11.2
	High	500	543	8.6	10.5	7.5
	Low	20	21	5.0	13.6	9.3
8-MQ-5-hmdCTP	Medium	100	111	11.0	7.7	9.5
	High	500	463	-7.4	10.4	7.3
	Low	20	22	10.0	10.7	7.8
8-MQ-N^1-meATP	Medium	100	109	9.0	10.7	9.5
	High	500	552	10.4	10.6	4.8
	Low	20	21	5.0	3.3	5.6
8-MQ-N^6-meATP	Medium	100	102	2.0	5.9	10.4
	High	500	522	4.4	6.5	12.6
	Low	20	21	5.0	11.4	10.3
8-MQ-2'-*O*-meATP	Medium	100	112	12.0	12.8	11.2
	High	500	483	-3.4	10.9	13.9
	Low	20	19	-5.0	5.2	3.9
8-MQ-2'-*O*-meGTP	Medium	100	111	11.0	9.9	4.9
	High	500	544	8.8	10.5	6.9
	Low	20	22	10.0	9.8	9.2
8-MQ-2-*S*-UTP	Medium	100	109	9.0	10.2	6.5
	High	500	562	12.4	11.2	5.9
	Low	20	18	-10.0	5.7	9.7
8-MQ-5-meCTP	Medium	100	113	13.0	9.4	8.8
	High	500	488	-2.4	8.9	7.7
	Low	20	19	-5.0	11.5	4.4
8-MQ-5-hmCTP	Medium	100	111	11.0	12.6	5.9
	High	500	552	10.4	13.8	6.8
	Low	20	21	5.0	9.8	8.7
8-MQ-7-meGTP	Medium	100	90	-10.0	3.9	6.4
	High	500	562	12.4	5.9	11.2
	Low	20	18	-10.0	6.7	9.6
8-MQ-ITP	Medium	100	109	9.0	6.7	6.8
	High	500	552	10.4	6.9	10.3
	Low	20	22	10.0	8.9	10.7
8-MQ-XTP	Medium	100	106	6.0	9.7	12.7
	High	500	542	8.4	8.9	11.8
	Low	20	18	-10.0	2.9	14.3
8-MQ-dATP	Medium	100	89	-11.0	8.3	12.2
	High	500	562	12.4	13.2	9.5
	Low	20	18	-10.0	11.2	10.4
8-MQ-dCTP	Medium	100	112	12.0	10.9	10.9
	High	500	569	13.8	12.3	12.4
	Low	20	19	-5.0	6.7	10.4
8-MQ-dGTP	Medium	100	112	12.0	8.9	9.8
	High	500	522	4.4	10.3	10.3
	Low	20	19	-5.0	14.7	6.7
8-MQ-TTP	Medium	100	91	-9.0	6.9	9.2
	High	500	433	-13.4	3.4	8.7
	Low	20	22	10.0	6.9	4.4
8-MQ-ATP	Medium	100	109	9.0	10.2	5.9
	High	500	476	-4.8	11.9	4.6
	Low	20	19	-5.0	4.5	10.6
8-MQ-CTP	Medium	100	91	-9.0	6.2	6.6
	High	500	555	11.0	8.7	14.8
	Low	20	21	5.0	13.4	13.2
8-MQ-GTP	Medium	100	112	12.0	8.9	11.3
	High	500	522	4.4	7.8	10.7
	Low	20	19	-5.0	12.4	11.2
8-MQ-UTP	Medium	100	114	14.0	12.4	12.9
	High	500	476	-4.8	14.9	12.3

Figure S1. The chemical structures of the 34 NTPs.

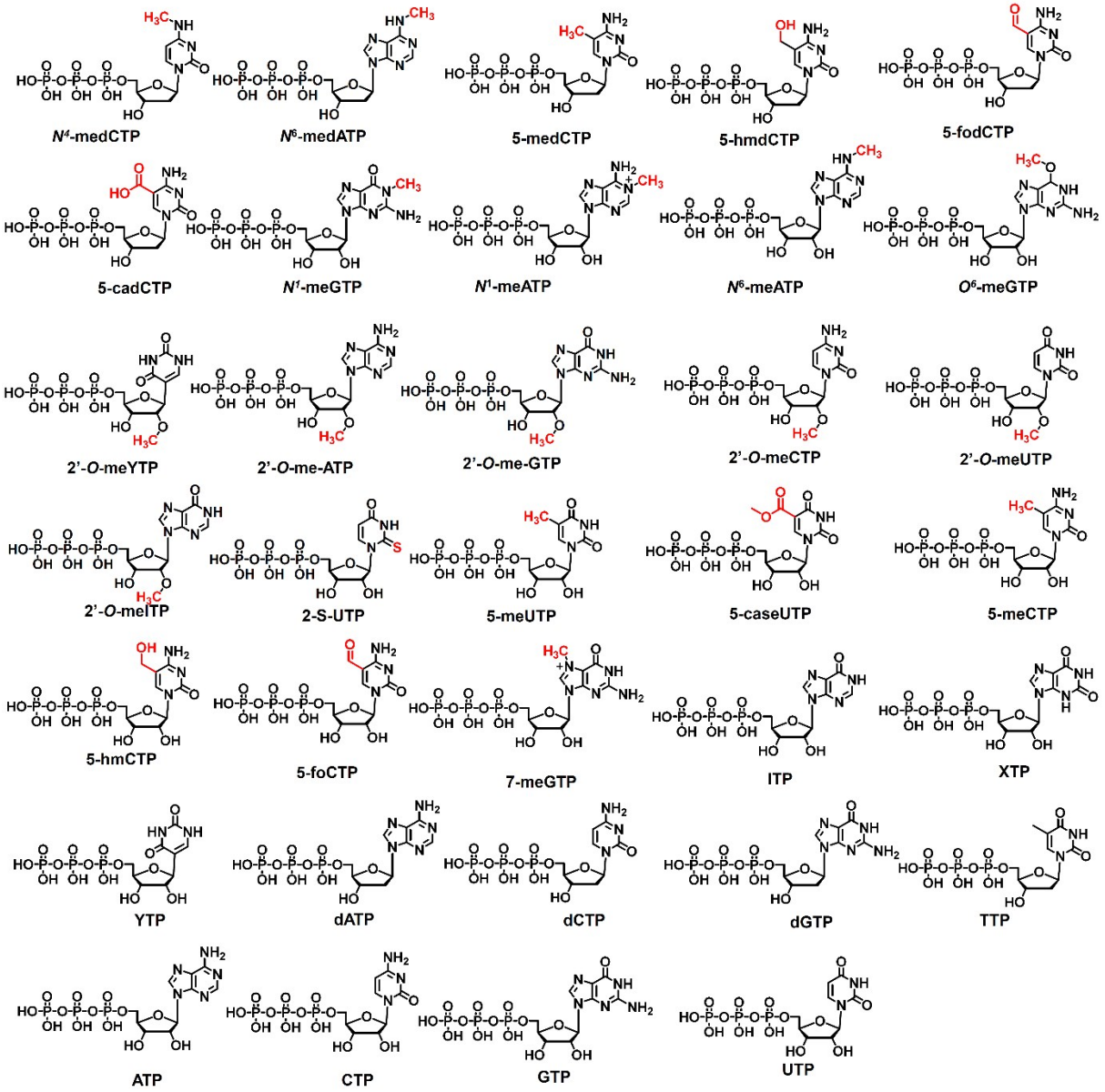

Figure S2. (A) Synthesis route of the 8-DMQ. (B) Characterization of 8-DMQ by the high-resolution mass spectrometry. Highlighted in red in (B) are the theoretical *m/z*.

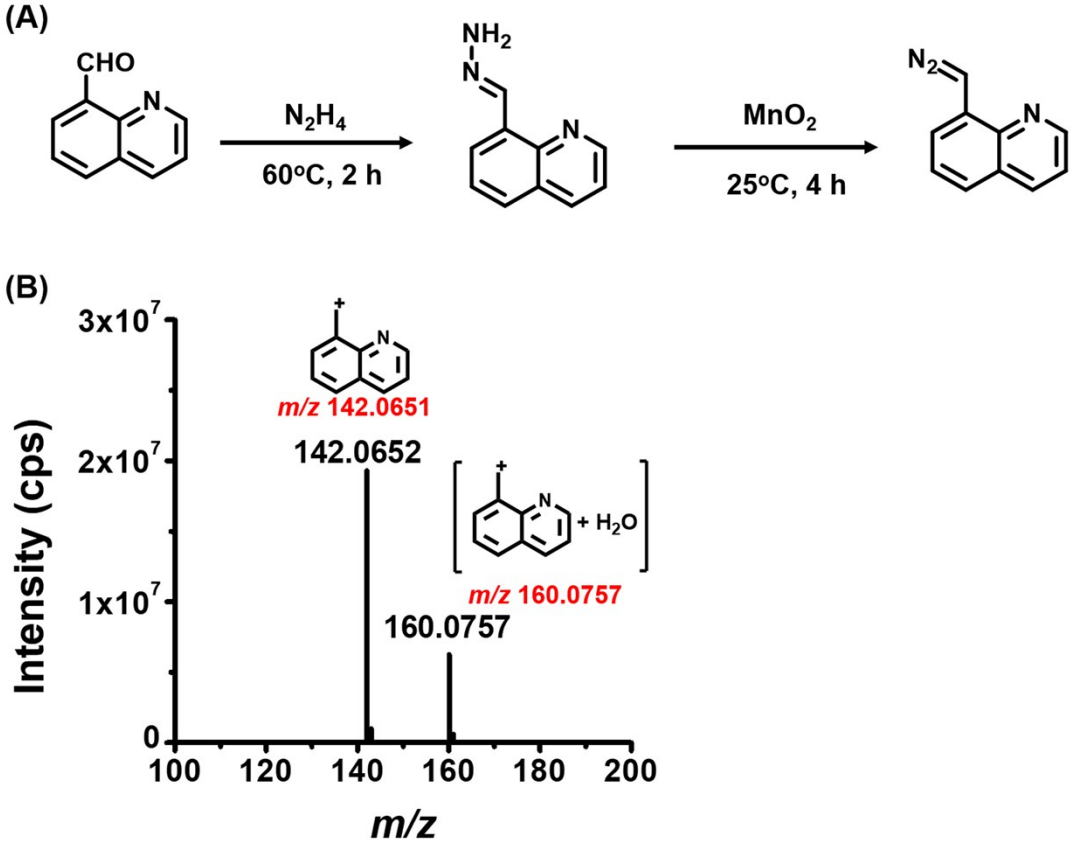

Figure S3. Characterization of the synthesized compounds by NMR. (A) The starting material of quinoline-8-carbaldehyde. (B) The product of 8-(hydrazonomethyl)quinolone from the first step synthesis. (C) 8-DMQ.

(A) The starting material of quinoline-8-carbaldehyde.

^{1}H NMR (400 MHz, DMSO-d_6) δ 11.35 (s, 1H), 9.12 (dd, J = 4.2, 1.8 Hz, 1H), 8.56 (dd, J = 8.4, 1.8 Hz, 1H), 8.38 (dd, J = 8.2, 1.6 Hz, 1H), 8.24 (dd, J = 7.2, 1.5 Hz, 1H), 7.82-7.78 (m, 1H), 7.72 (dd, J = 8.4, 4.2 Hz, 1H).

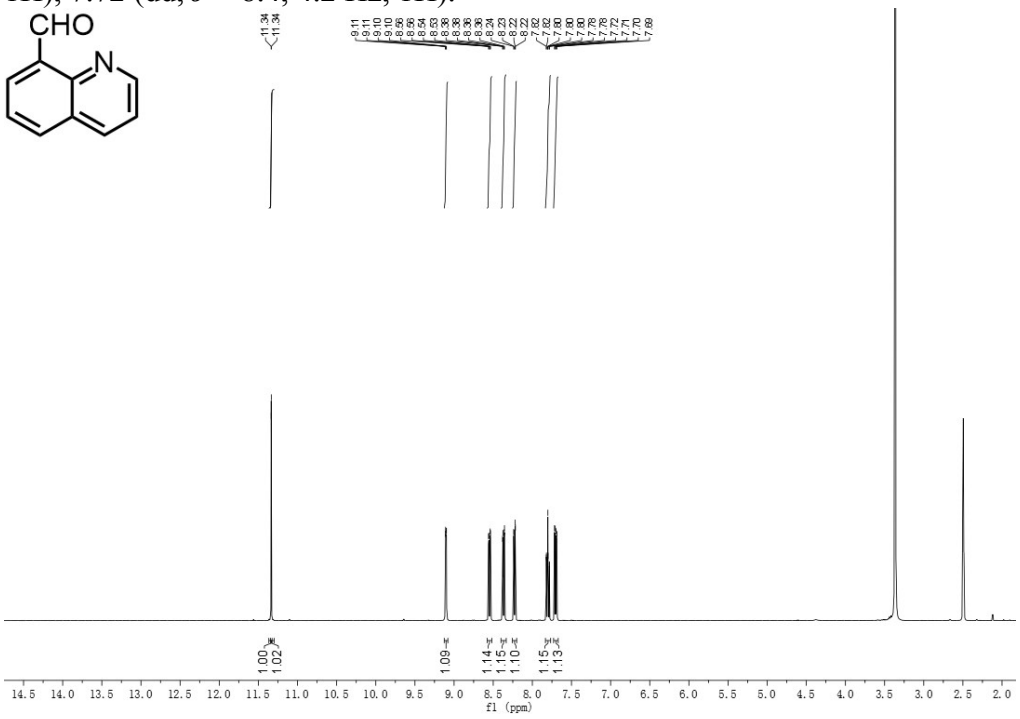

^{13}C NMR (101 MHz, DMSO-d_6) δ 192.1, 151.9, 146.8, 136.9, 135.0, 131.0, 128.8, 128.1, 126.4, 122.4.

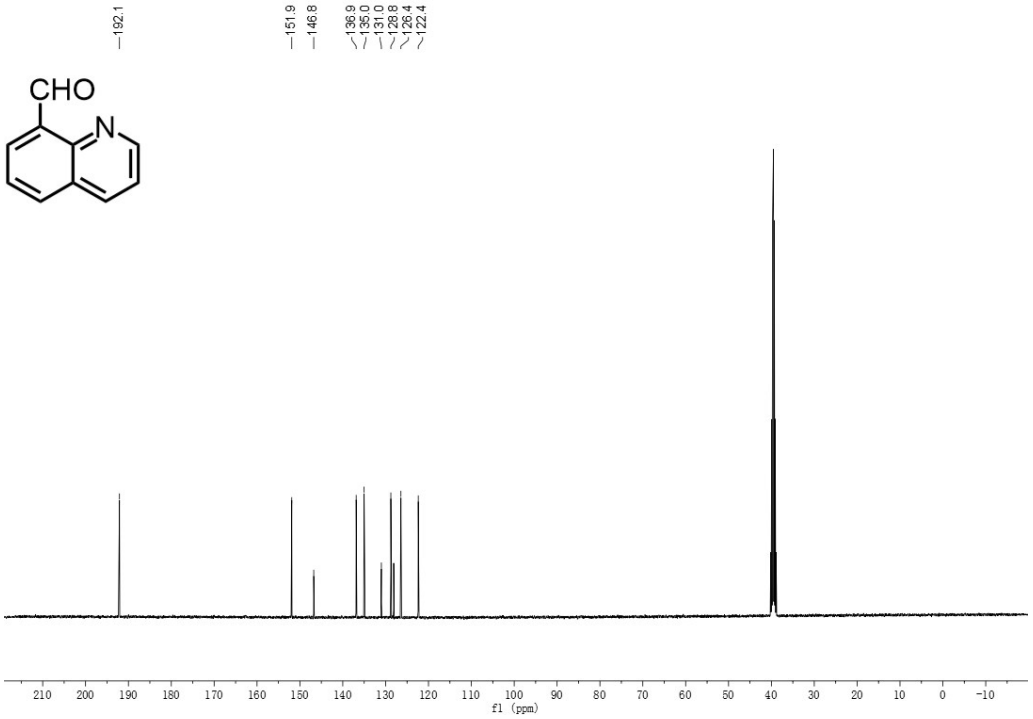

(B) The product of 8-(hydrazonomethyl)quinolone from the first step synthesis.
^{1}H NMR (400 MHz, DMSO-d_6) δ 8.94 (s, 1H), 8.91 (dd, J = 4.1, 1.8 Hz, 1H), 8.36 (dd, J = 8.3, 1.8 Hz, 1H), 8.12 (dd, J = 7.4, 1.5 Hz, 1H), 7.86 (dd, J = 8.1, 1.5 Hz, 1H), 7.61 – 7.51 (m, 2H), 7.10 (s, 2H).

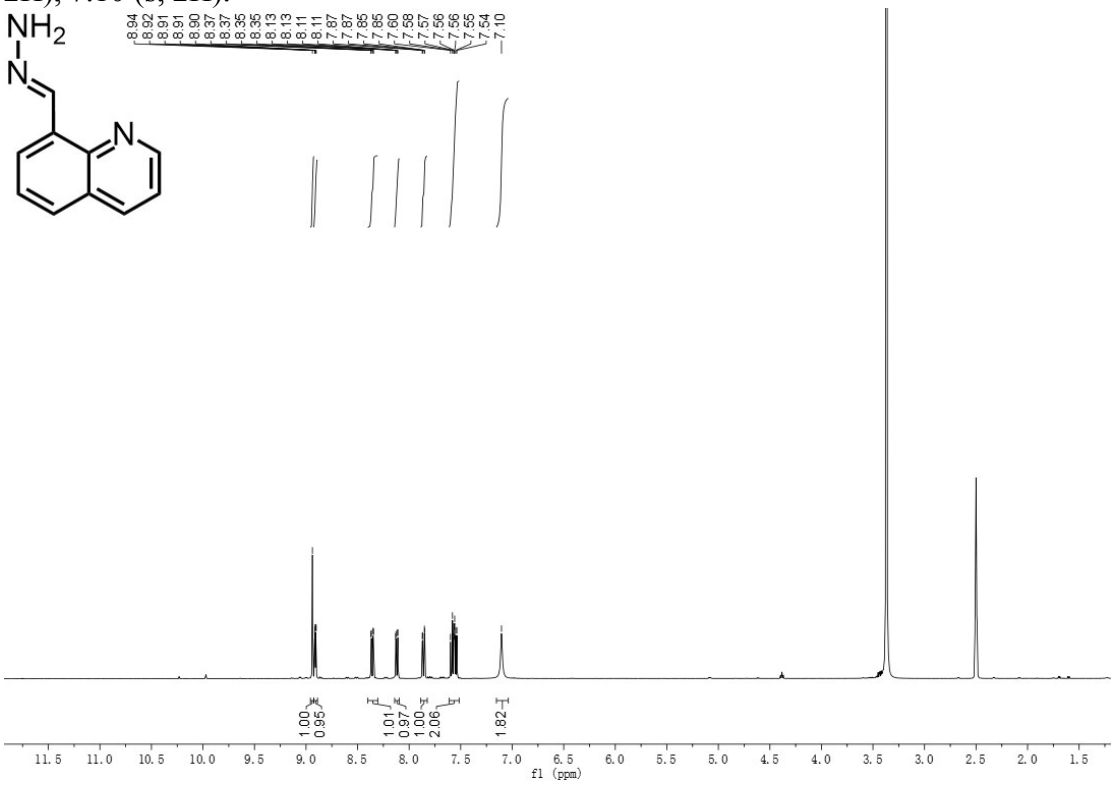

^{13}C NMR (101 MHz, DMSO-d_6) δ 149.6, 144.5, 136.4, 134.7, 133.4, 128.1, 127.0, 126.6, 123.4, 121.5.

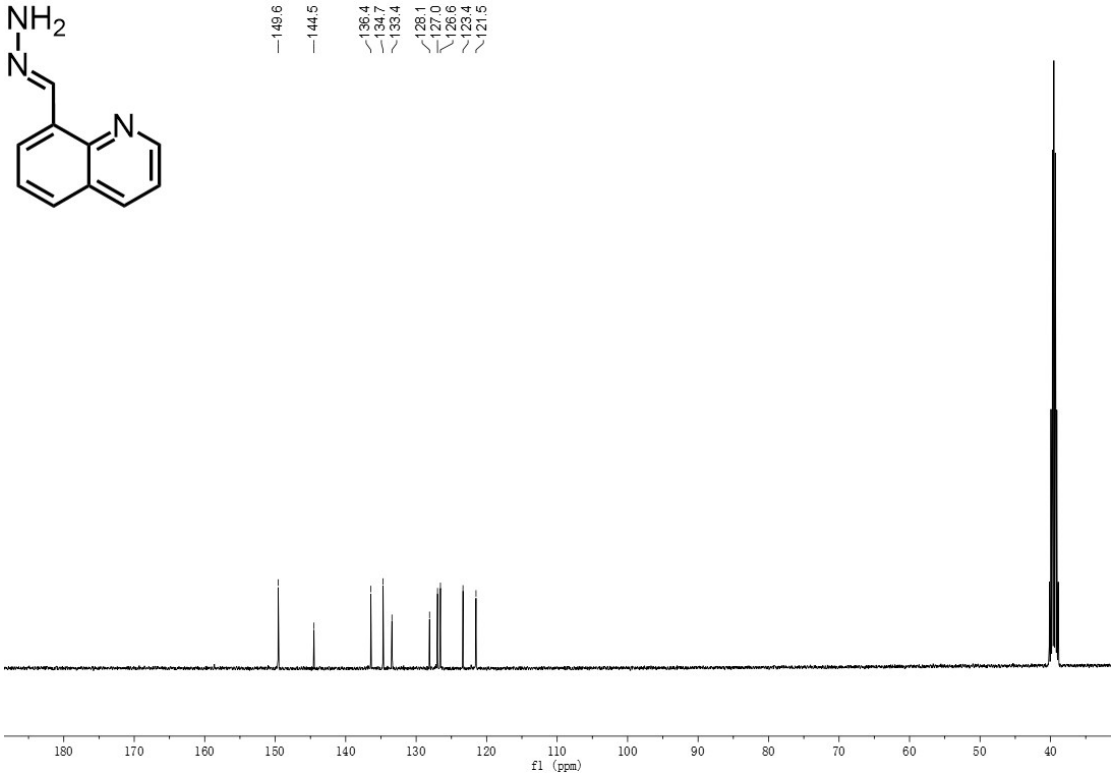

(C) 8-DMQ.

^{1}H NMR (400 MHz, DMSO-d_6) δ 8.82 (s, 1H), 8.32 (d, J = 8.5 Hz, 1H), 7.60-7.51 (m, 3H), 7.26 (d, J = 7.2 Hz, 1H), 6.44 (s, 1H).

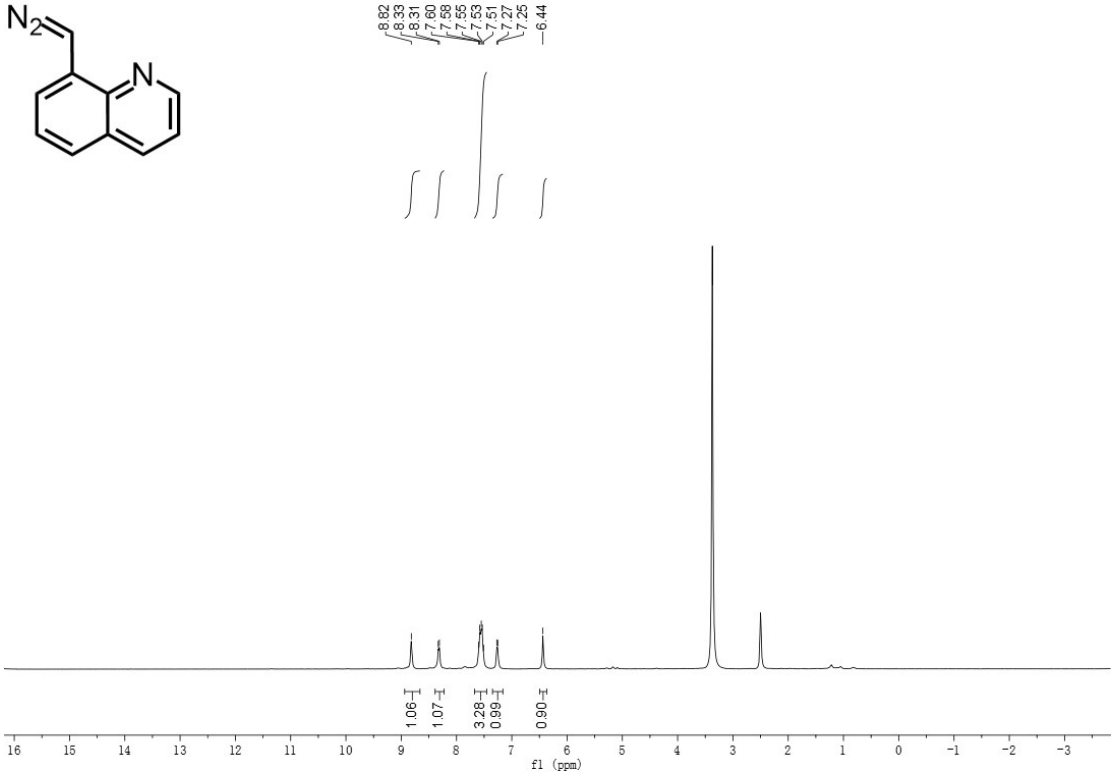

^{13}C NMR (101 MHz, DMSO-d_6) δ 148.8, 142.5, 136.5, 128.9, 128.4, 126.9, 122.6, 122.0, 119.9, 43.9.

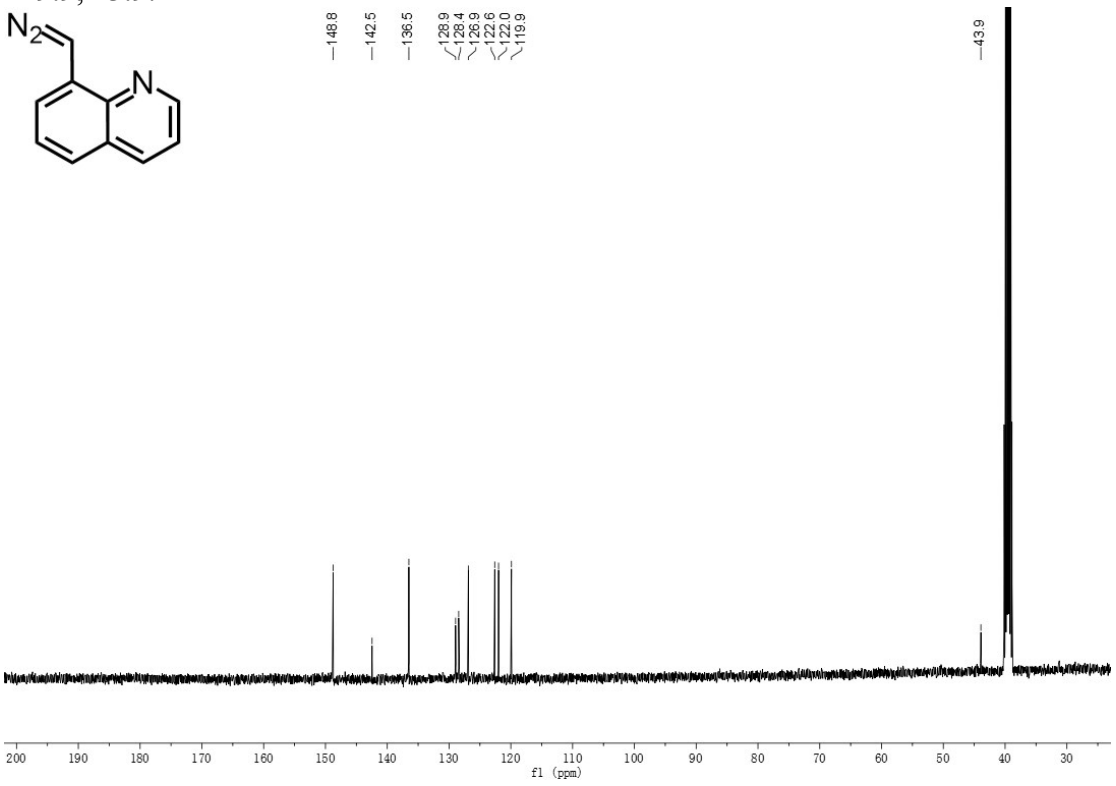

Figure S4. LC chromatograms of synthetic compounds. (A) Quinoline-8-carbaldehyde. (B) Purified 8-(hydrazonomethyl)quinolone. (C) Purified 8-DMQ. (D) Unpurified 8-DMQ. The synthetic compounds were analyzed on a Shimadzu LC-20AD HPLC system (Tokyo, Japan) with two 20AD pumps. An Accucore C18 column (150 mm × 2.1 mm i.d., 2.6 µm, Thermo Fisher Scientific, USA) was used for the separation. The column temperature was set at 35°C. 0.05% FA in water (solvent A) and methanol (solvent B) were employed as mobile phases. A gradient of 0 - 3 min 5% B, 3 - 5 min 5% to 12% B, 5 - 20 min 12% to 80% B and 20-25 min 80% B was used. The flow rate was set at 0.2 mL/min.

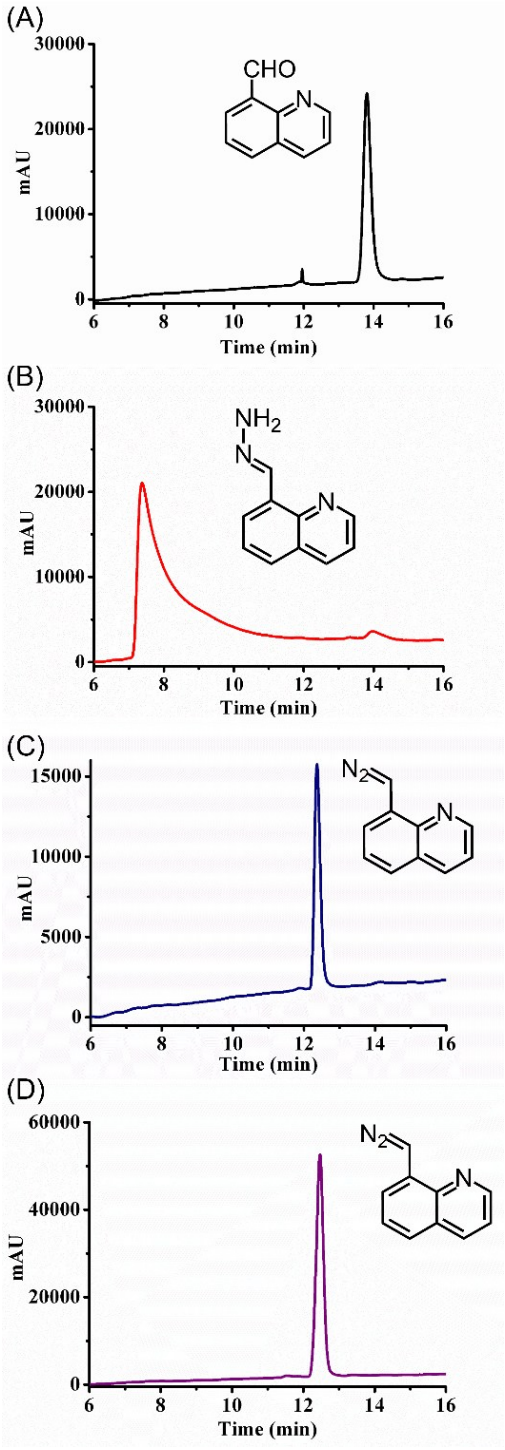

Figure S5. The extracted ion chromatograms, high-resolution MS spectra and product ions spectra of 8-DMQ-labeled 34 kinds of NTP standards.

1, ATP

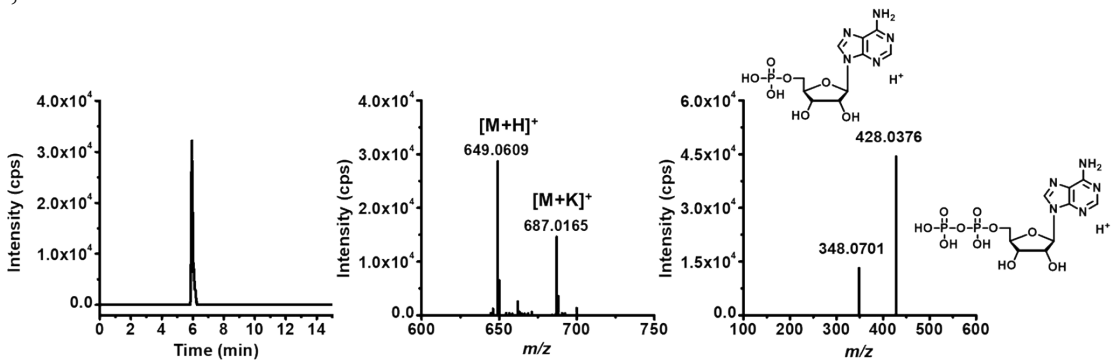

2, dATP

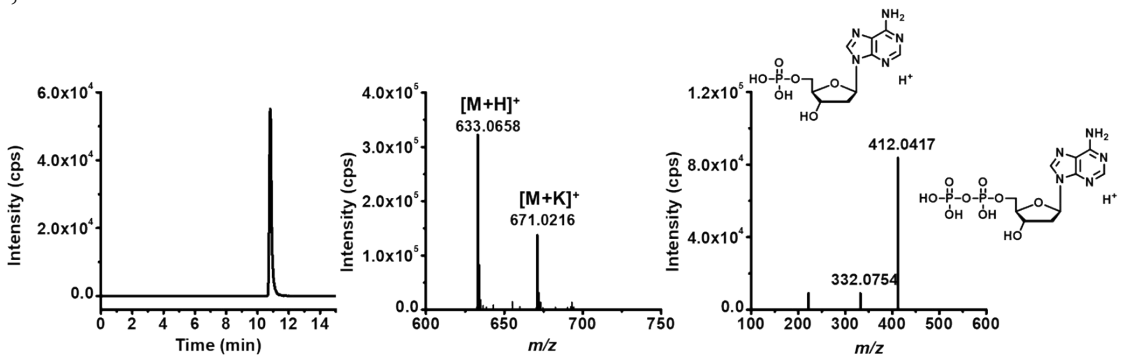

3, GTP

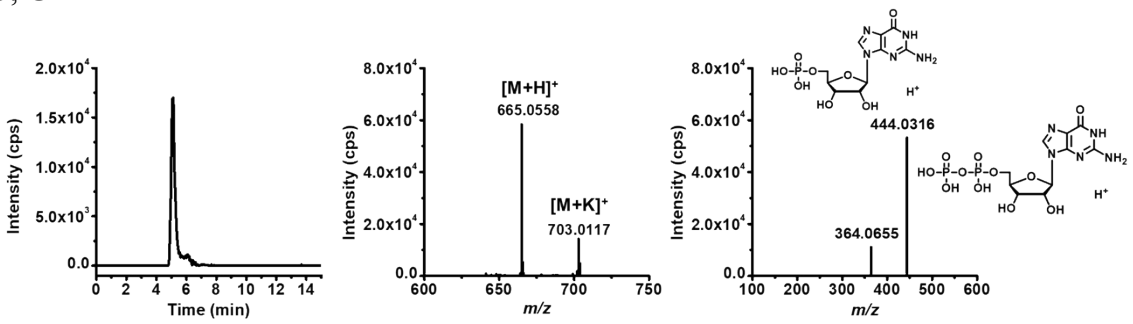

4, dGTP

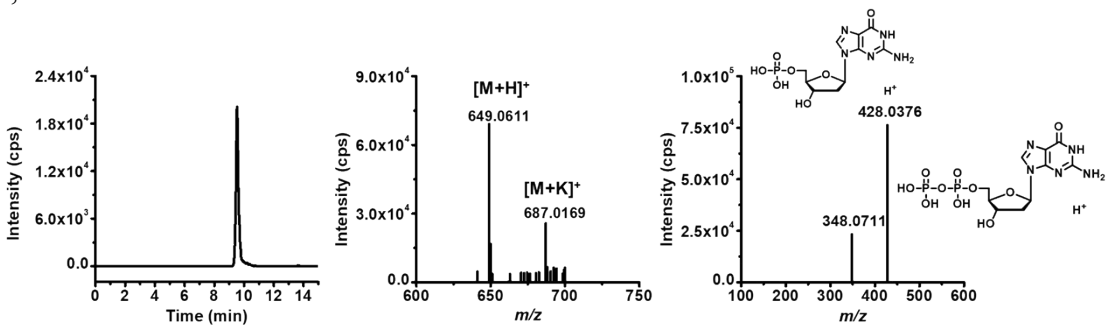

5, CTP;

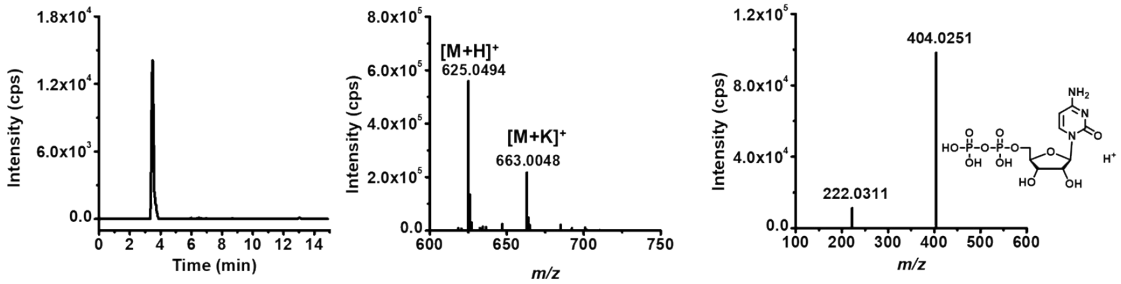

6, dCTP

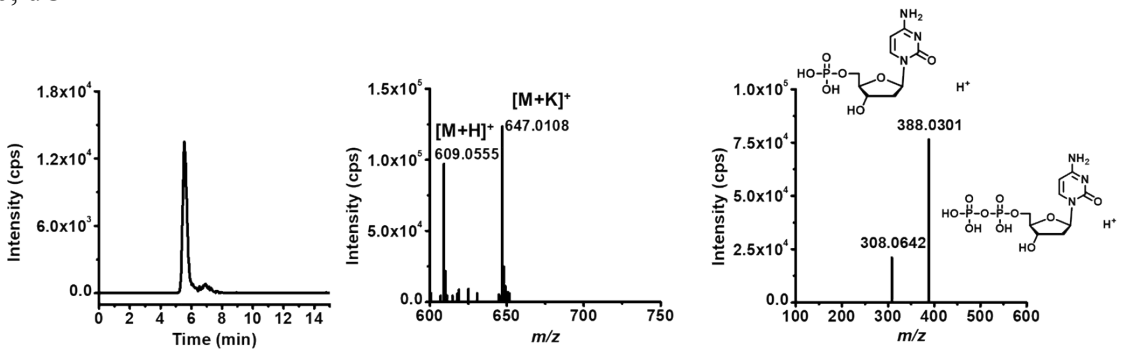

7, UTP

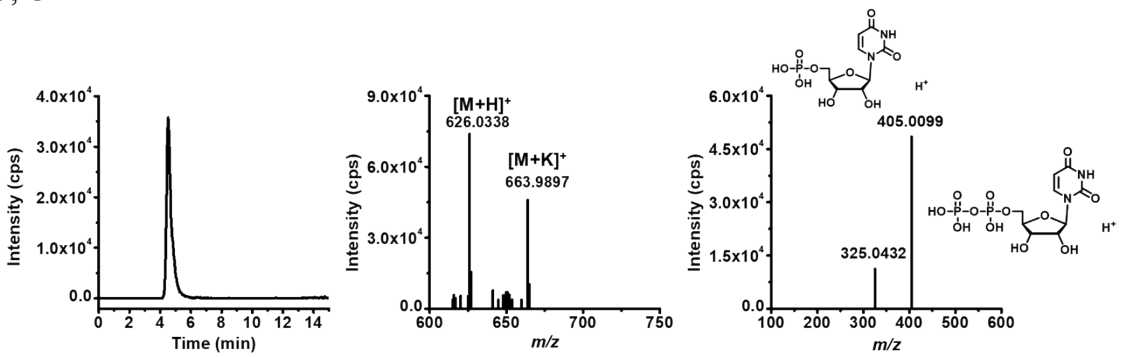

8, TTP

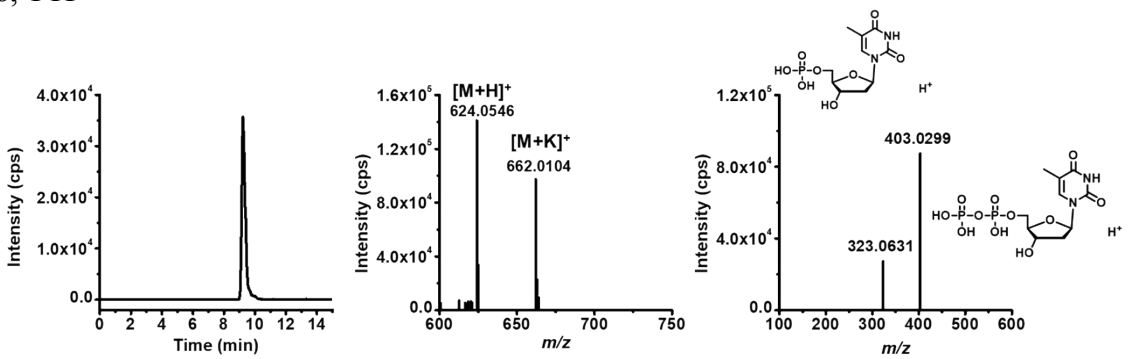

9, N^6-meATP

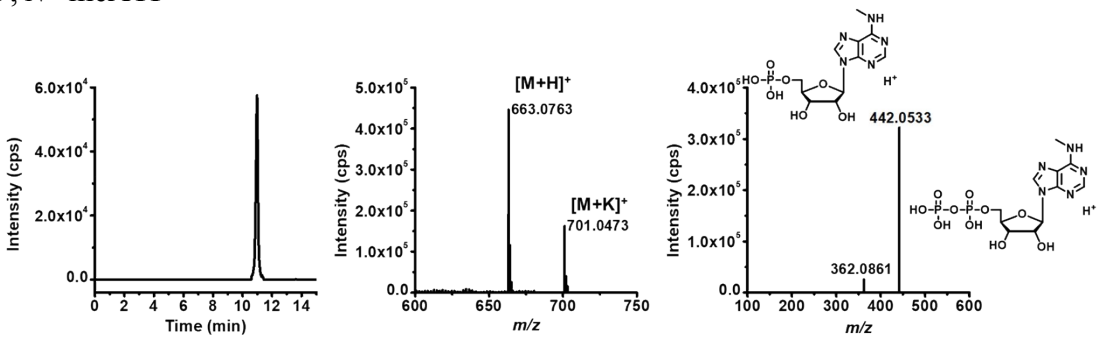

10, 7-meGTP

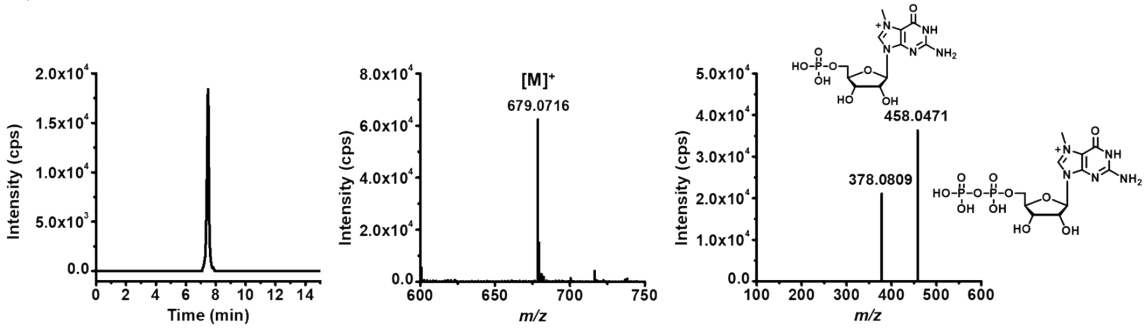

11, ITP

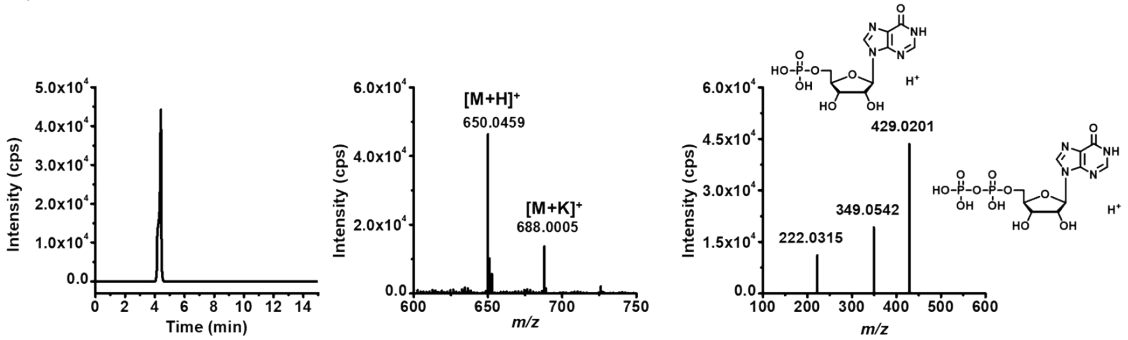

12, XTP

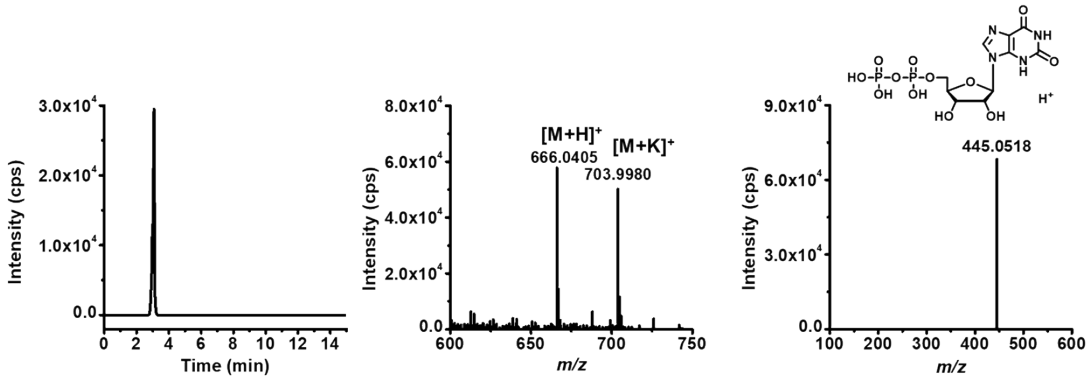

13, N^1-meATP

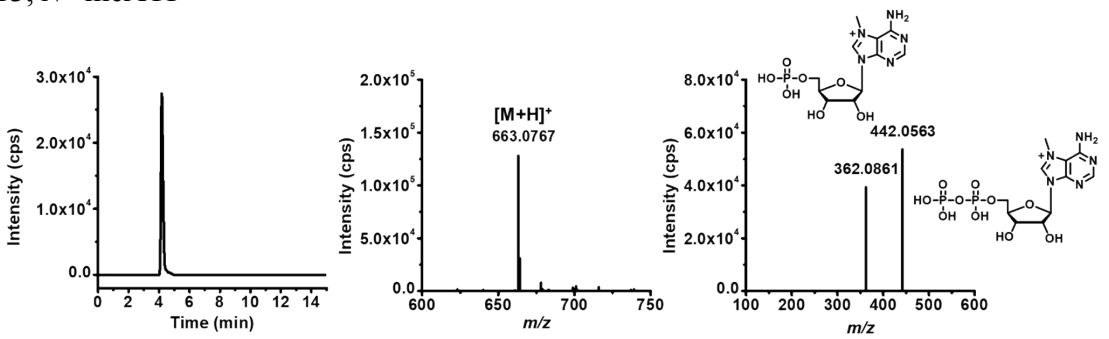

14, 2-*S*-UTP

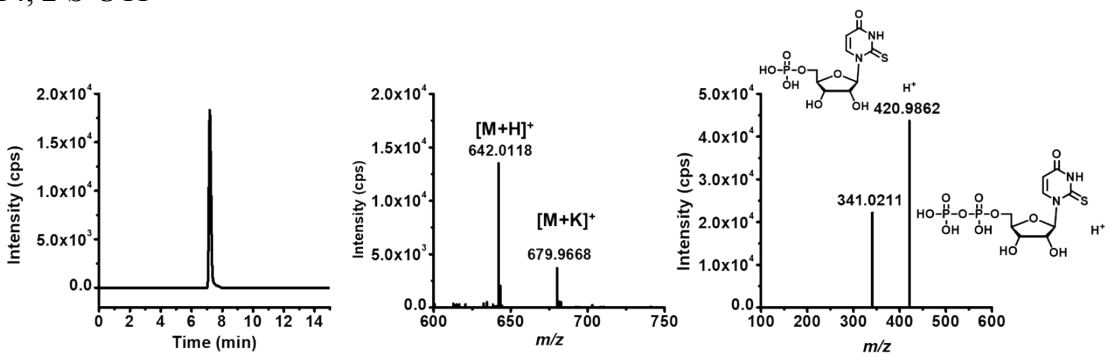

15, 5-hmCTP

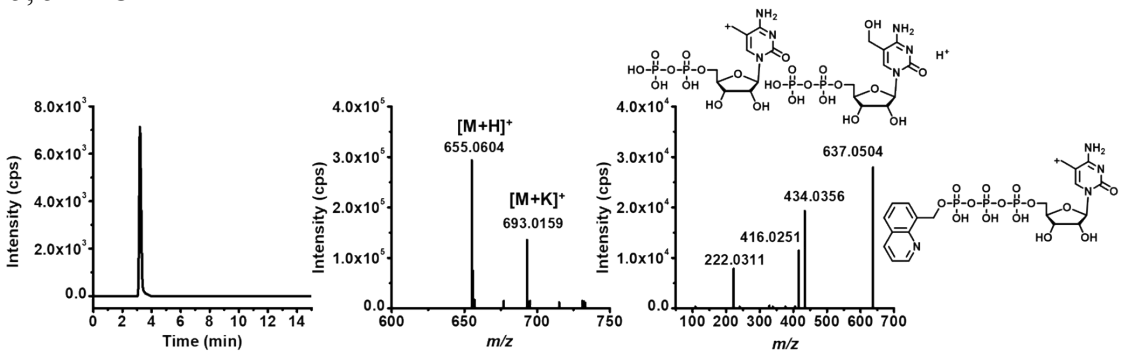

16, 5-meCTP

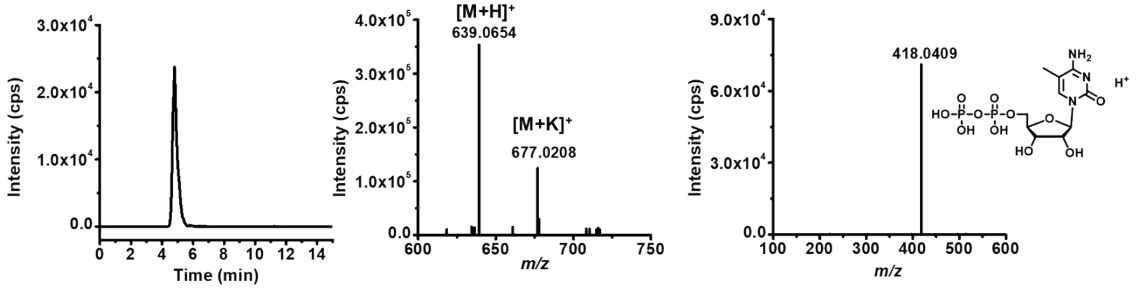

17, 5-medCTP

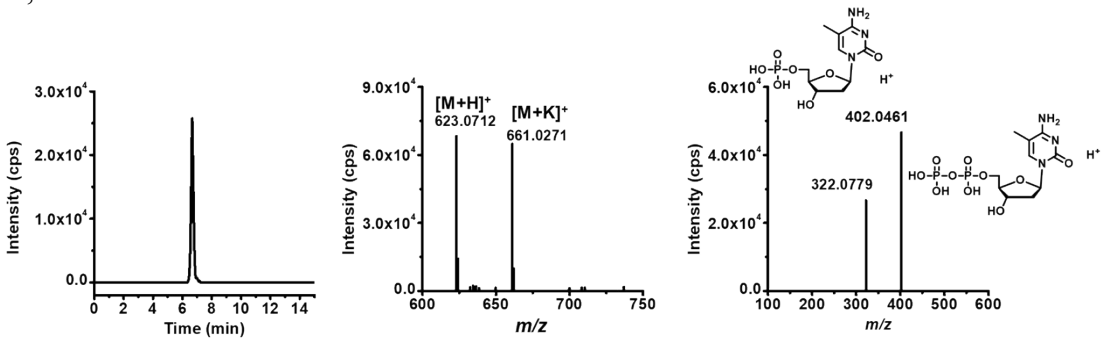

18, 5-hmdCTP

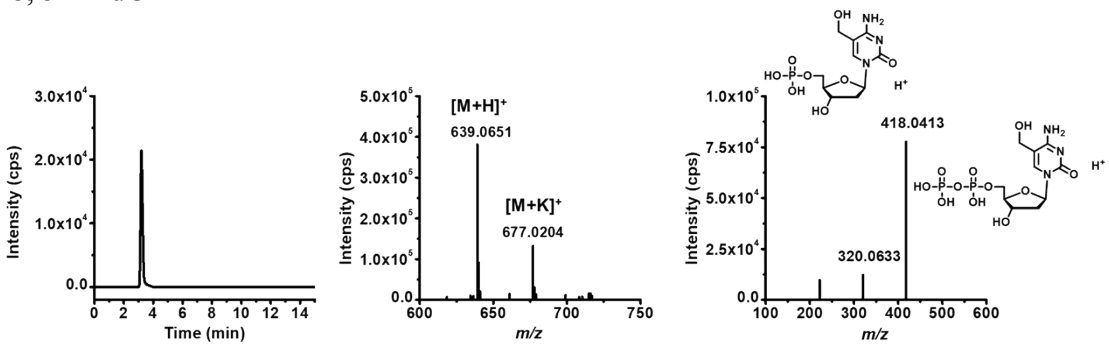

19, 2'-*O*-meATP

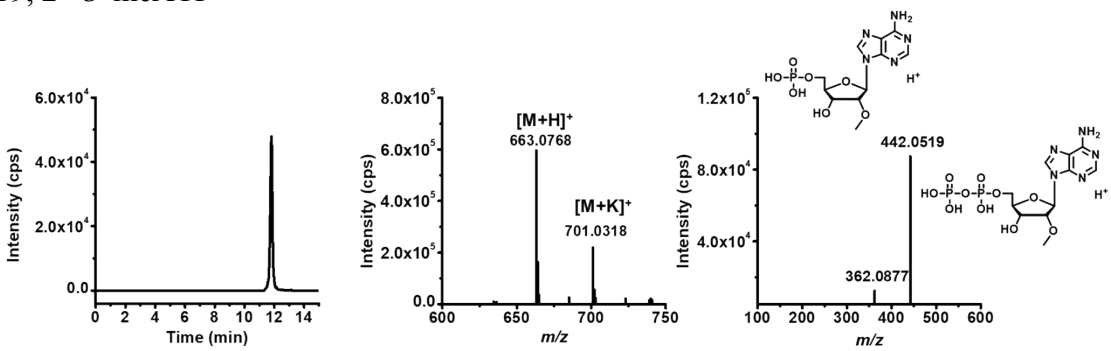

20, 2'-*O*-me-GTP

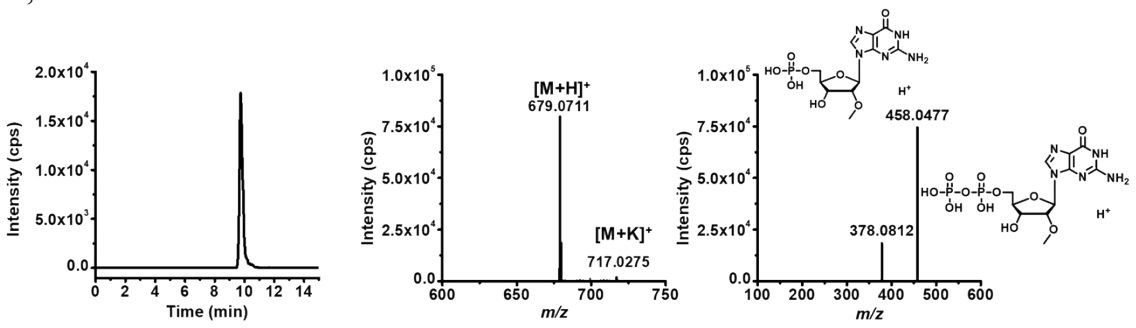

21, 5-cadCTP

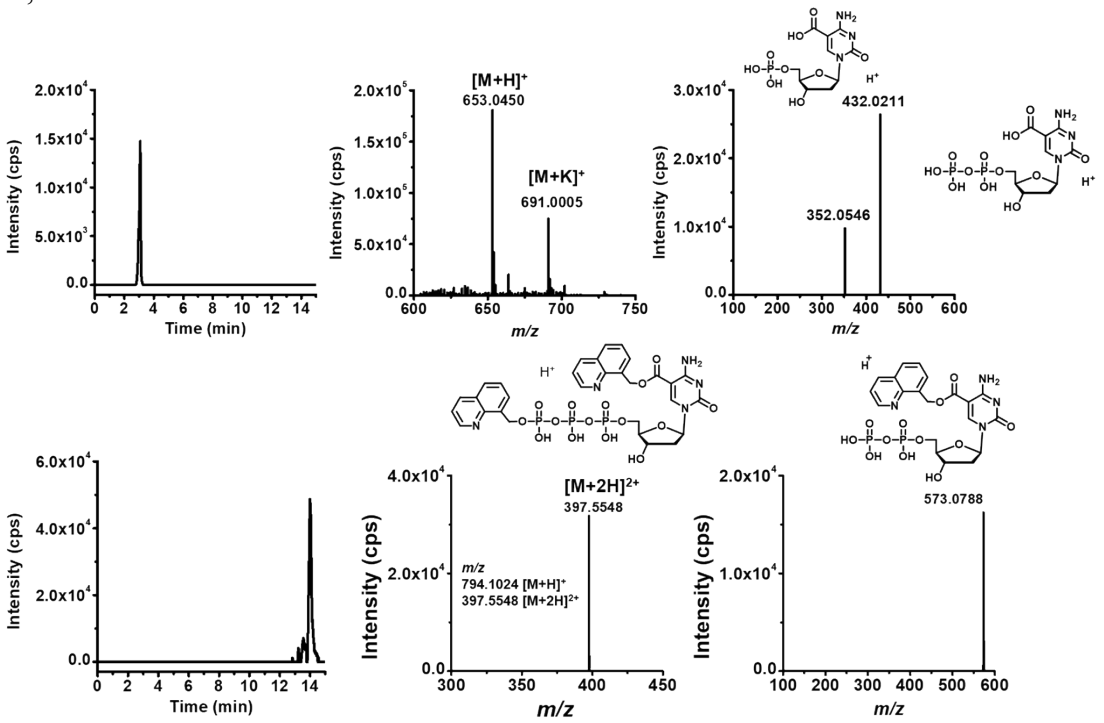

22, YTP

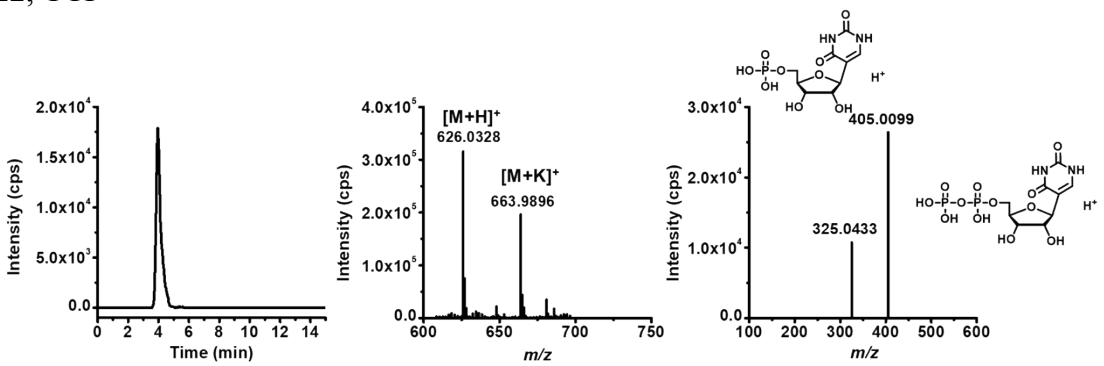

23, 2'-*O*-me-ITP

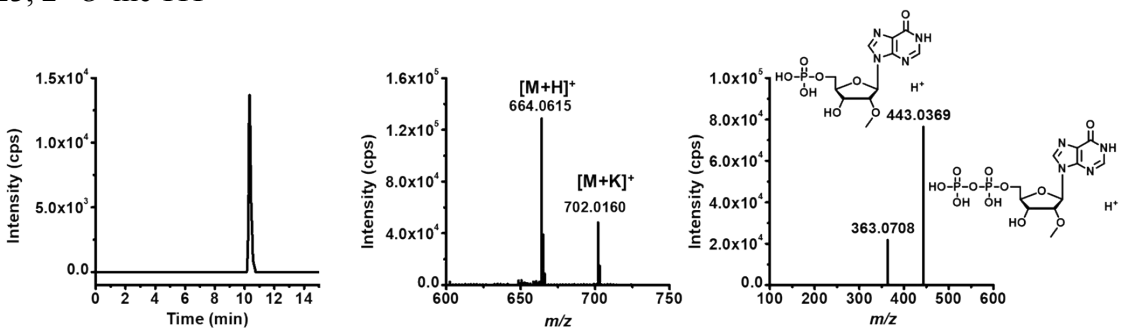

24, 5-meUTP

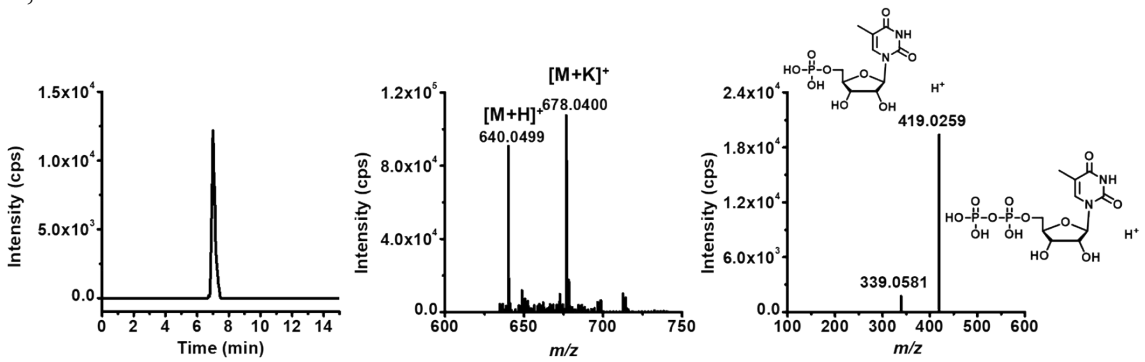

25, 2'-*O*-meCTP

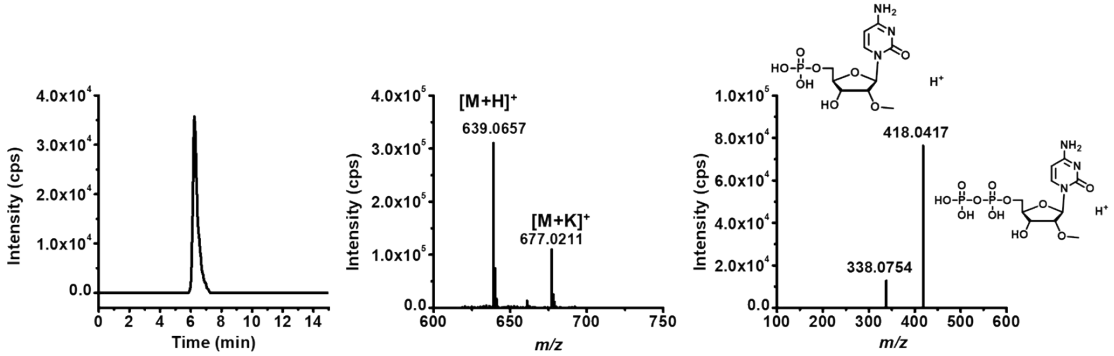

26, 5-caseUTP;

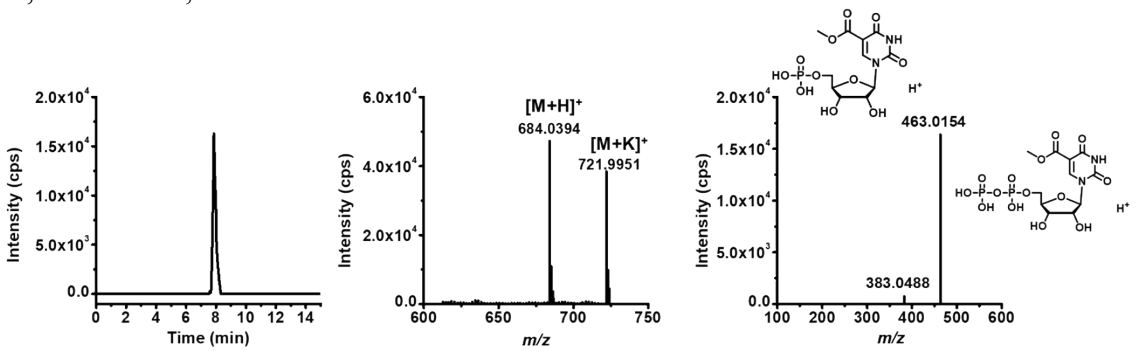

27, N^6-medATP

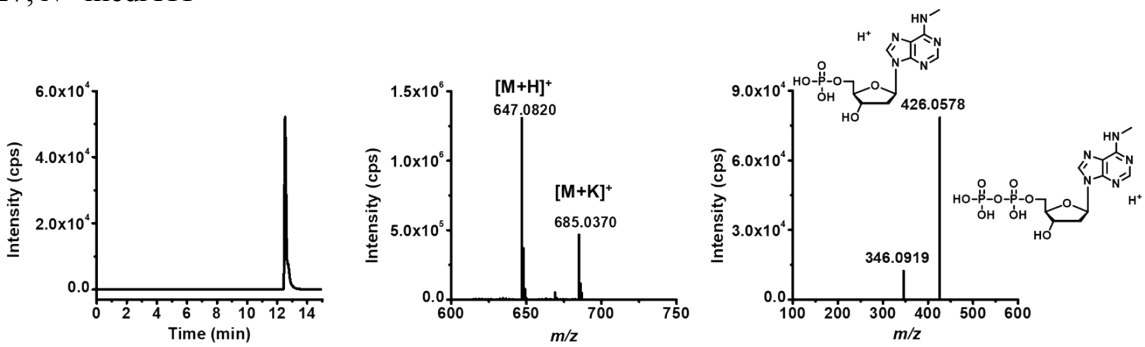

28, N^4-medCTP

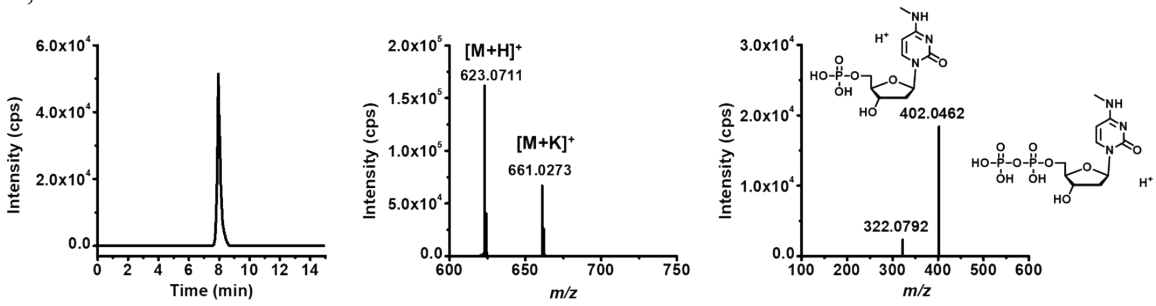

29, 2'-*O*-meYTP

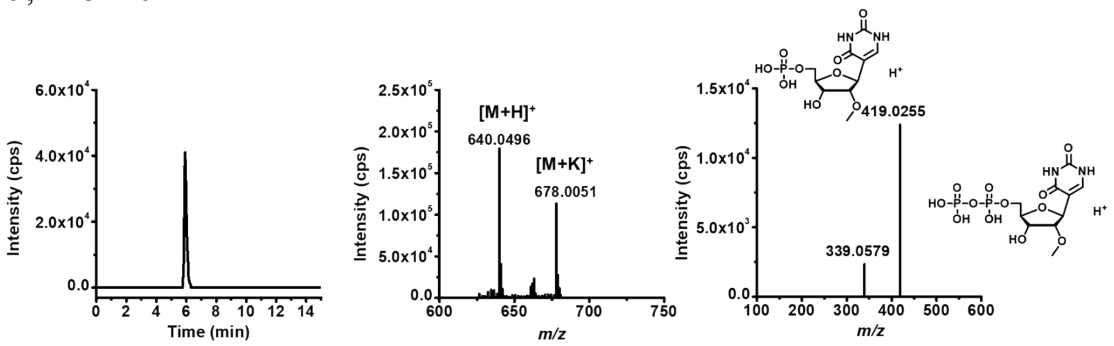

30, 2'-*O*-meUTP

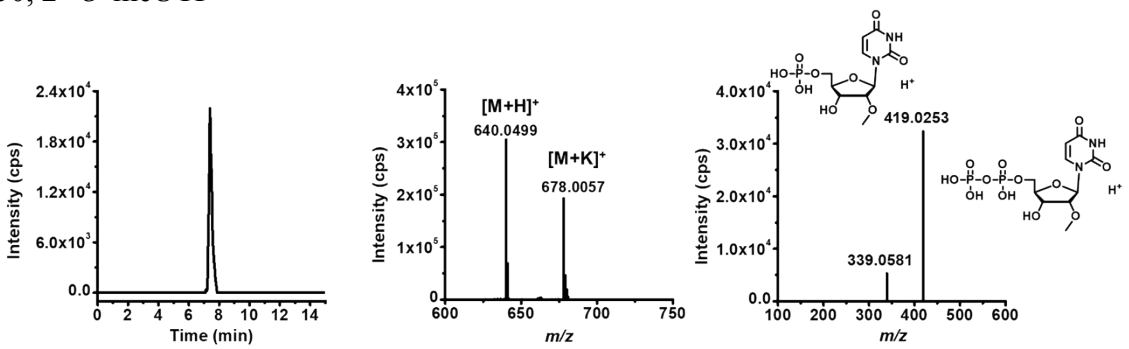

31, 5-fodCTP

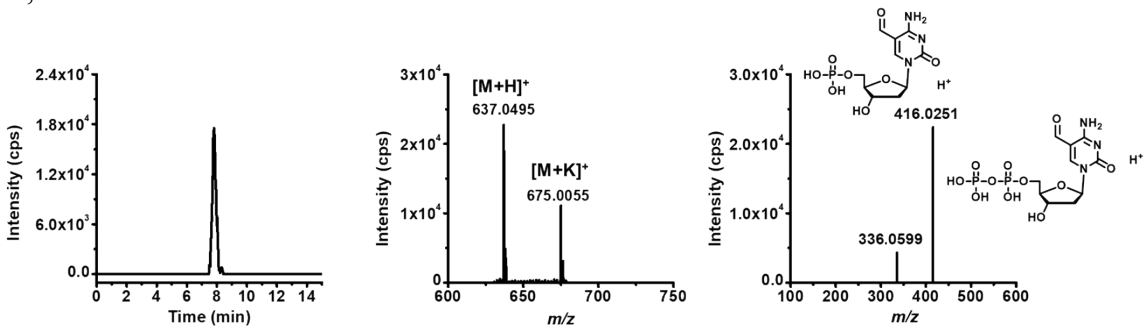

32, 5-foCTP

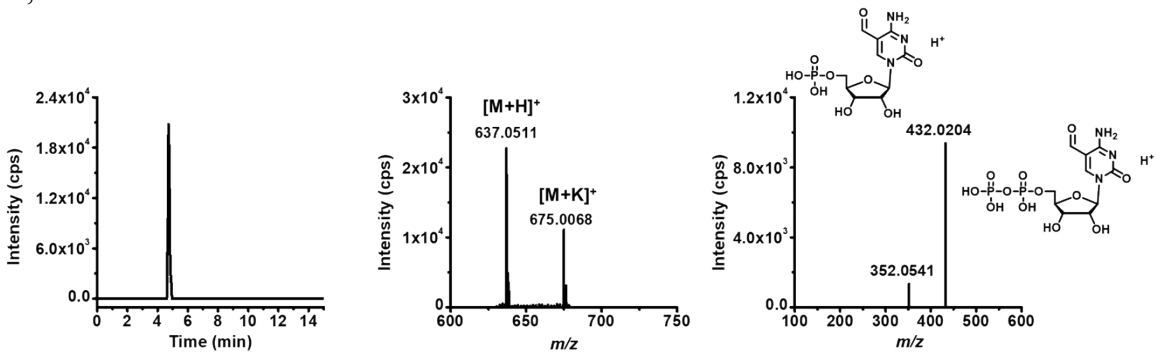

33, O^6-meGTP

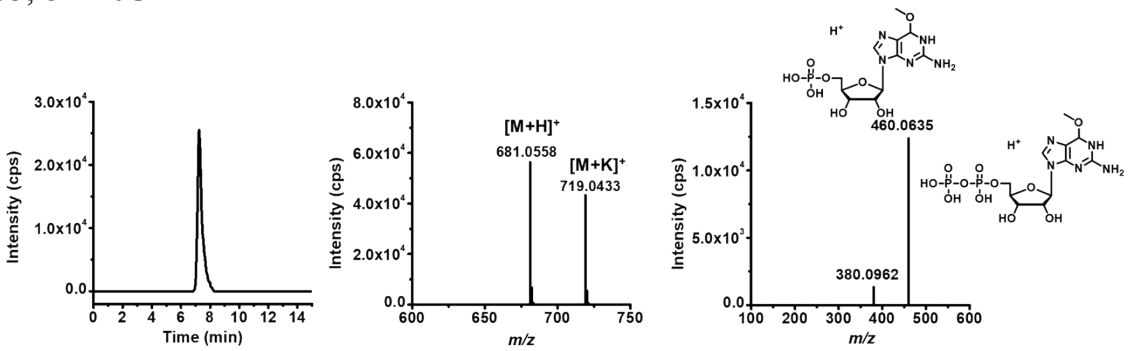

34, N^1-meGTP

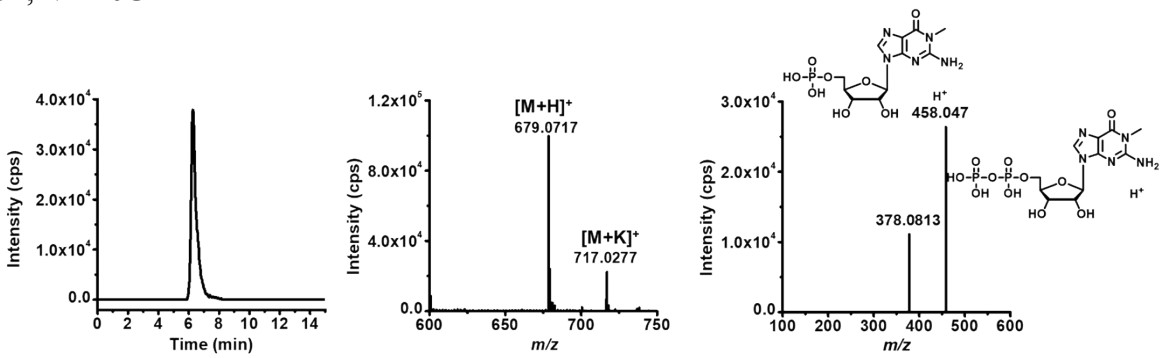

Figure S6. The mass spectra of ATP and dATP after 8-DMQ labeled. No additional peaks (double or triple labeling) were observed in these spectra, suggesting that only one phosphate group of NTPs could be labeled by 8-DMQ.

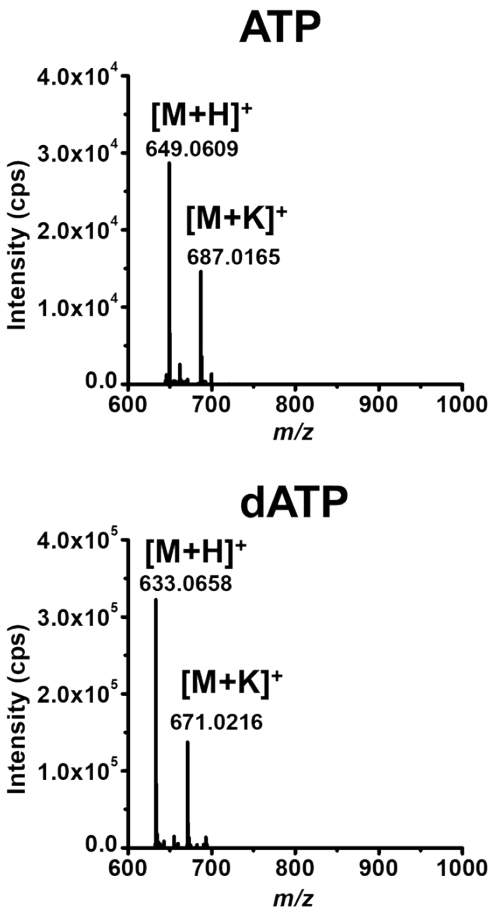

Figure S7. Evaluation of the stabilities of native NTPs and 8-DMQ-labeled NTPs (8-MQ-NTPs). NTPs and 8-MQ-NTPs were stored at 25°C for evaluation of the stabilities. The NTPs and 8-MQ-NTPs were analyzed by LC-ESI-MS/MS at the time points of 0.5 h, 1 h, 2 h, 5 h, and 10 h. 5 mM of NTPs were used for the evaluation.

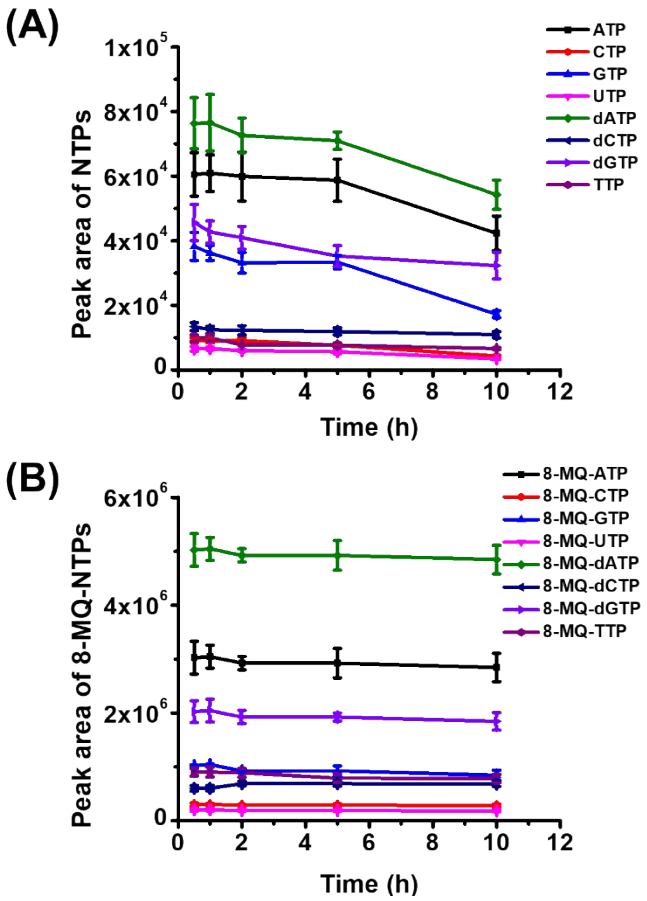

Figure S8. Optimization of reaction conditions of NTPs (8 canonical NTPs) by 8-DMQ. (A) Optimization of molar ratios of 8-DMQ over NTPs. (B) Optimization of reaction temperature. (C) Optimization of reaction time.

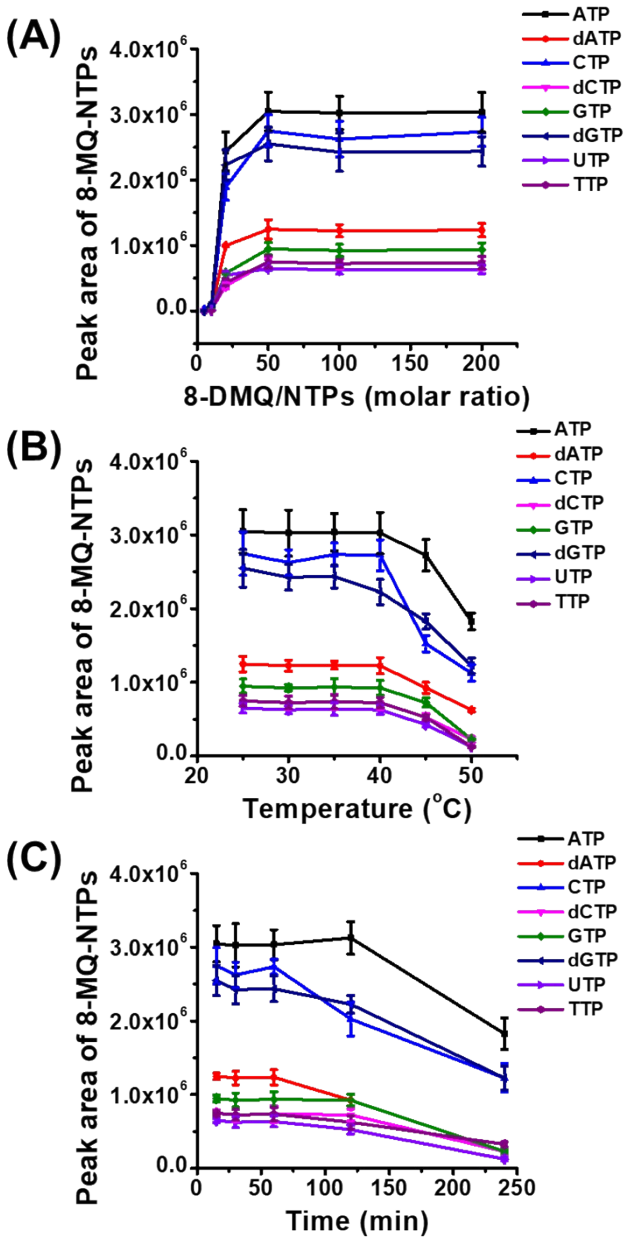

Figure S9. Evaluation of the chemical labeling reaction of NTPs by 8-DMQ. After 8-DMQ labeling, almost no residual NTPs were detectable, indicating the good labeling efficiencies by 8-DMQ.

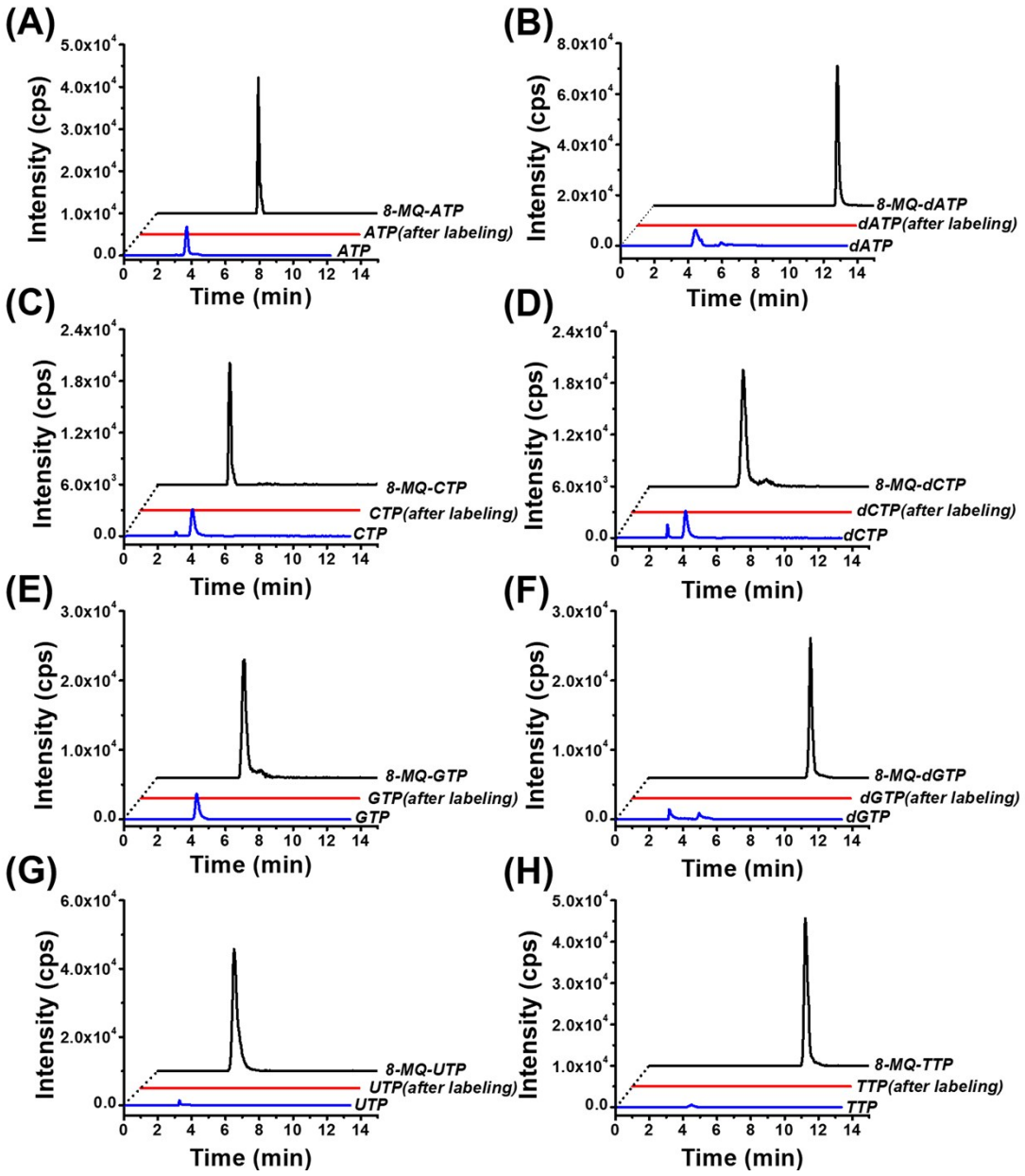

Figure S10. Identification of modified NTPs and canonical NTPs in 293T cells. (A) The extracted ion chromatograms (left panel), high-resolution MS spectra (middle panel) and product ions spectra (right panel) of standards. (B) The extracted ion chromatograms (left panel), high-resolution MS spectra (middle panel) and product ions spectra (right panel) of the compounds detected in 293T cells.

1. ATP

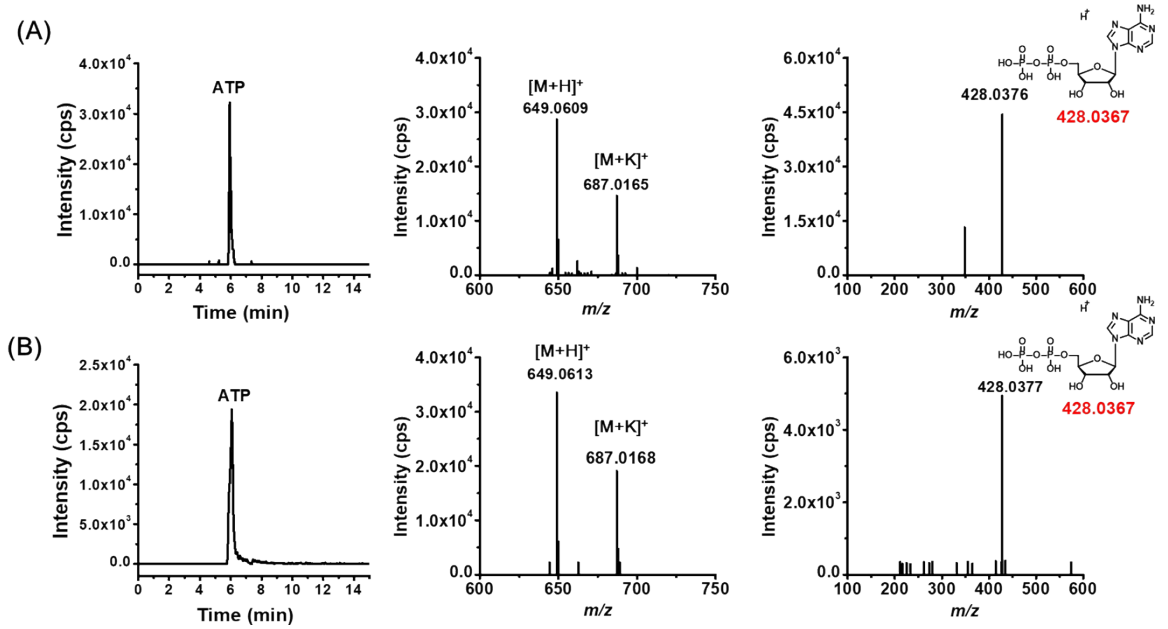

2. dATP

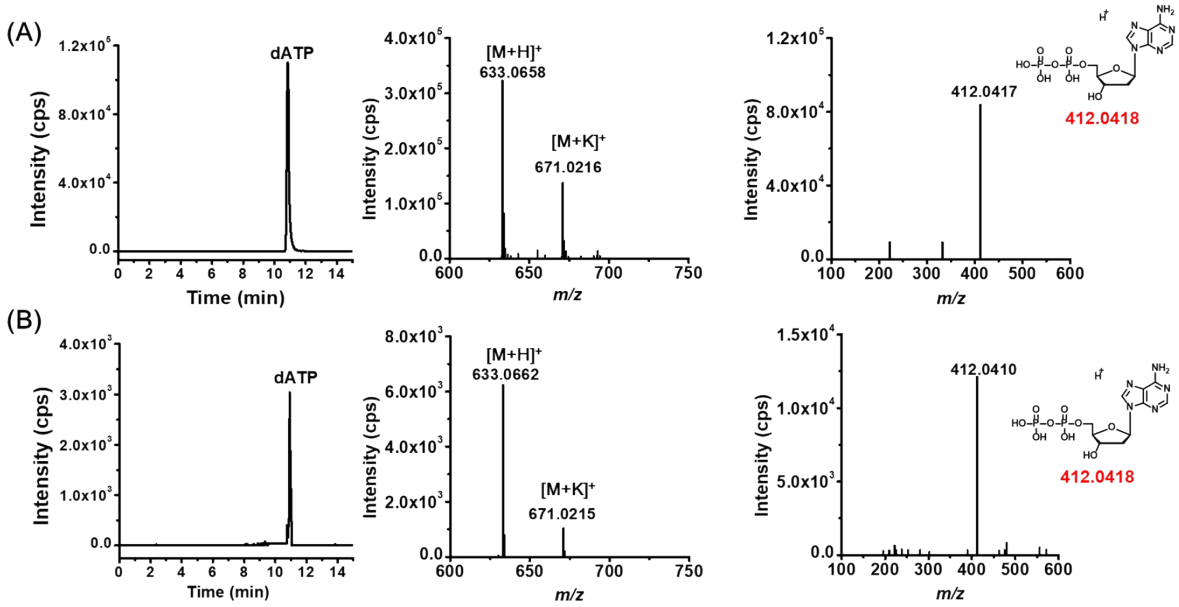

3. GTP

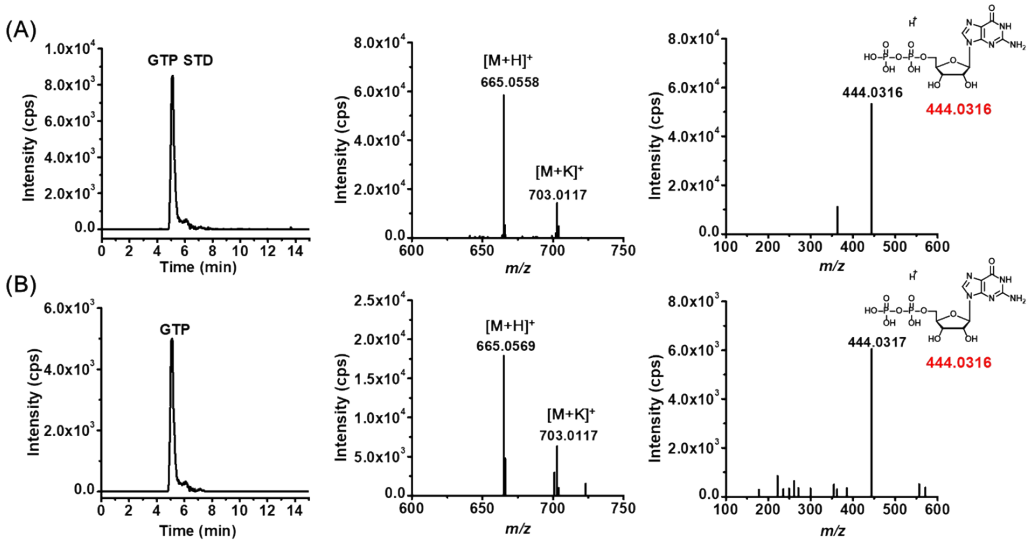

4. dGTP

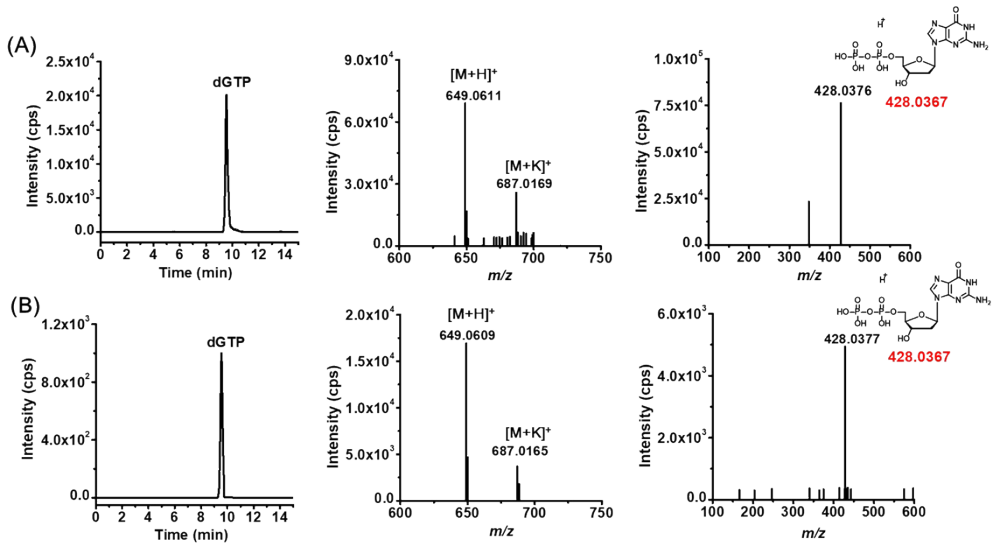

5. CTP

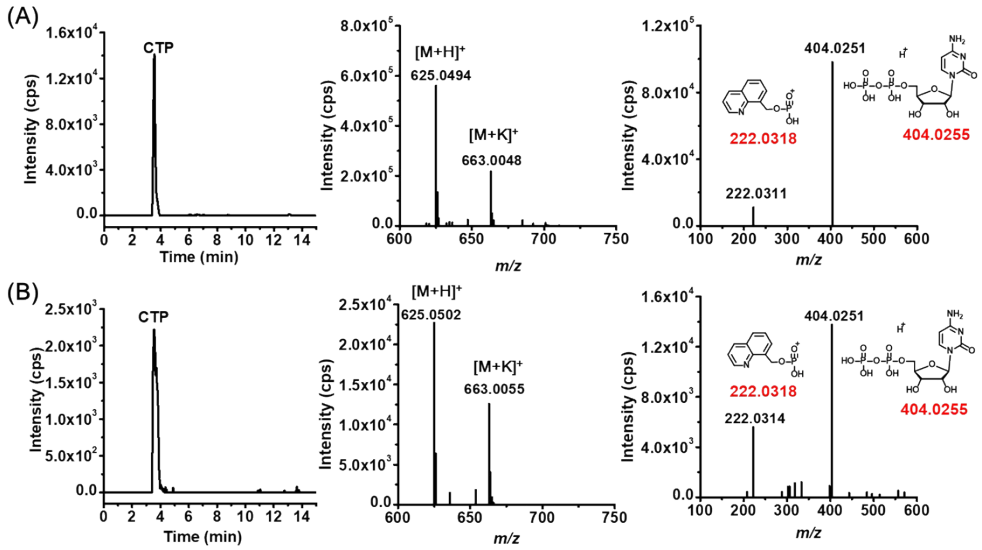

6. dCTP

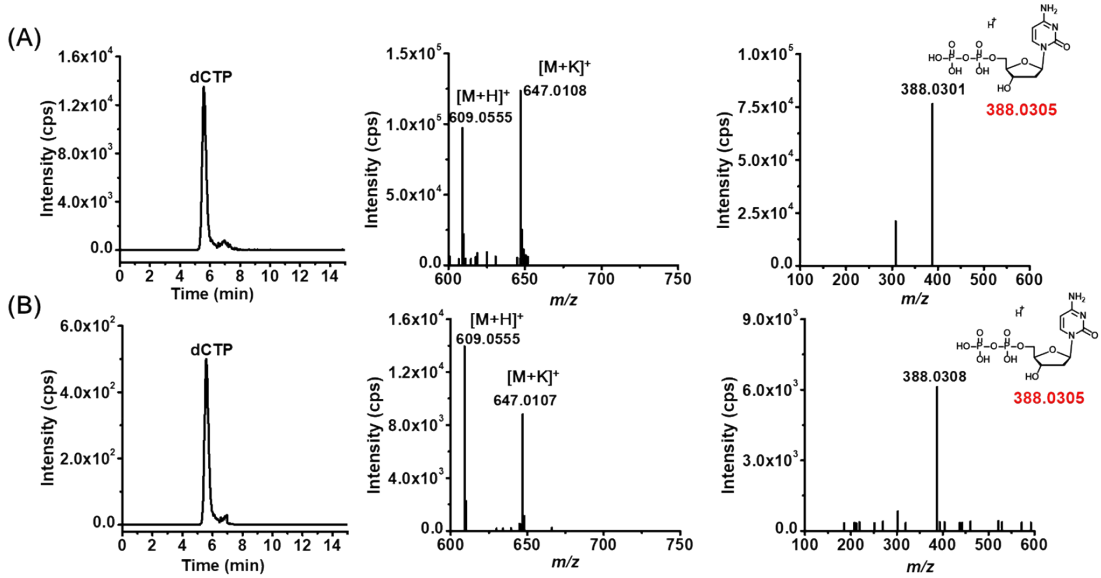

7. UTP

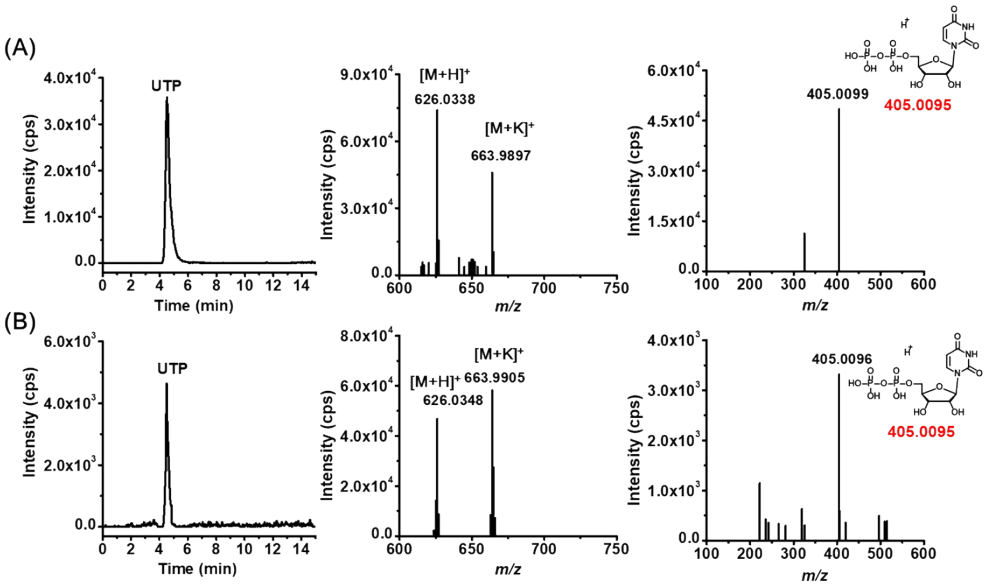

8. TTP

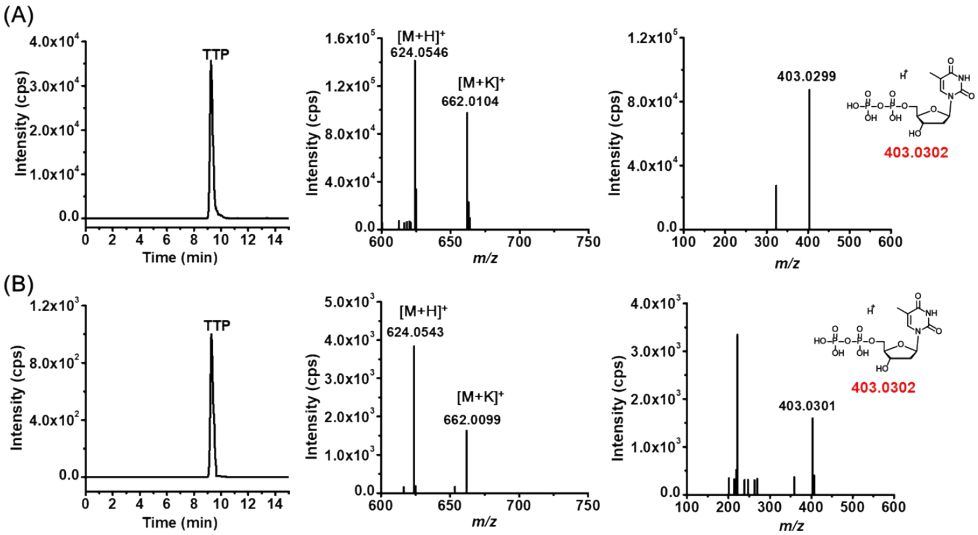

9. N^6-meATP

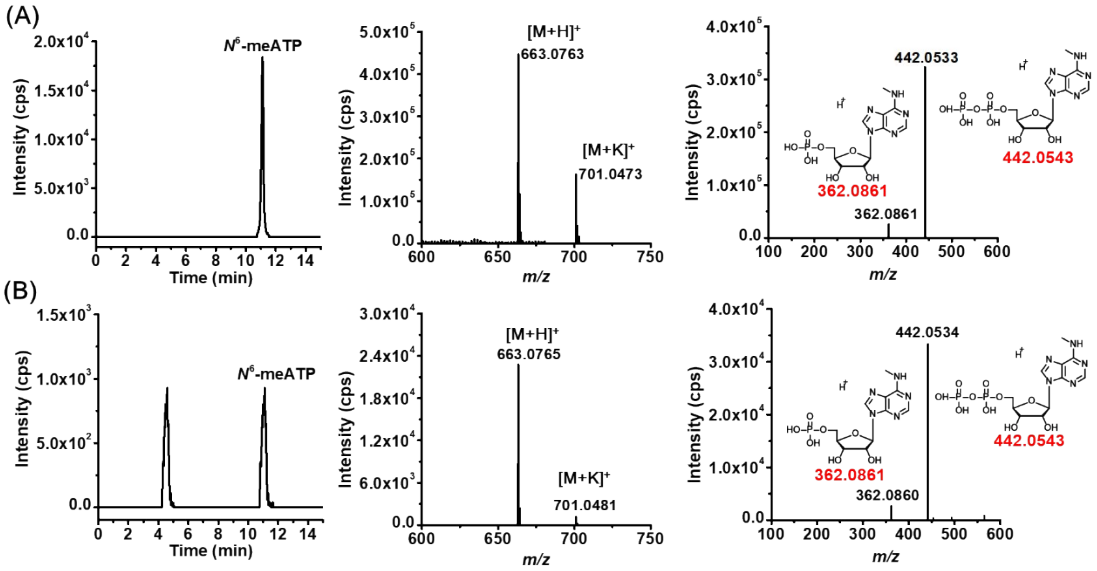

10. 7-meGTP

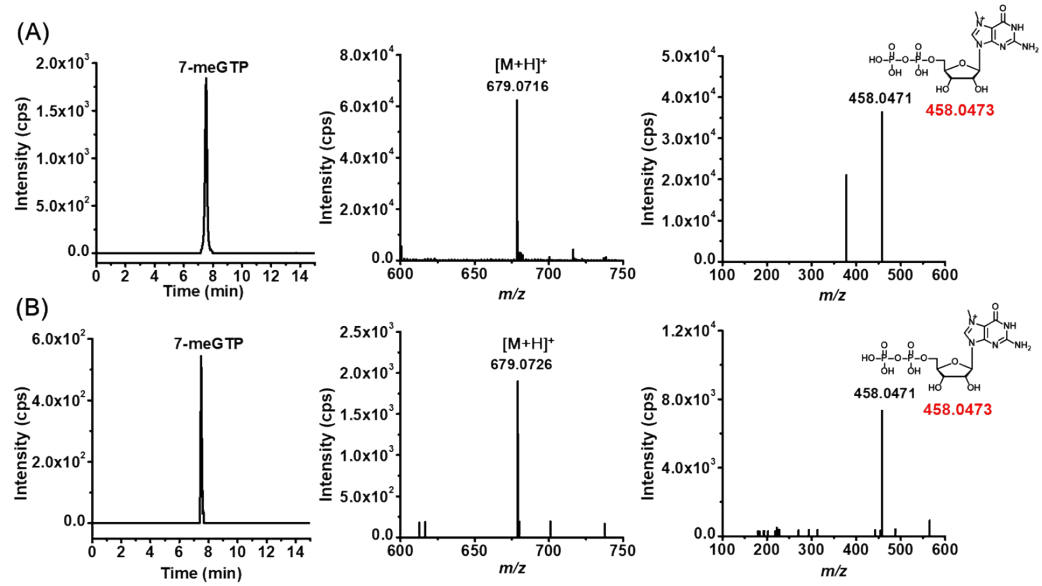

11. ITP

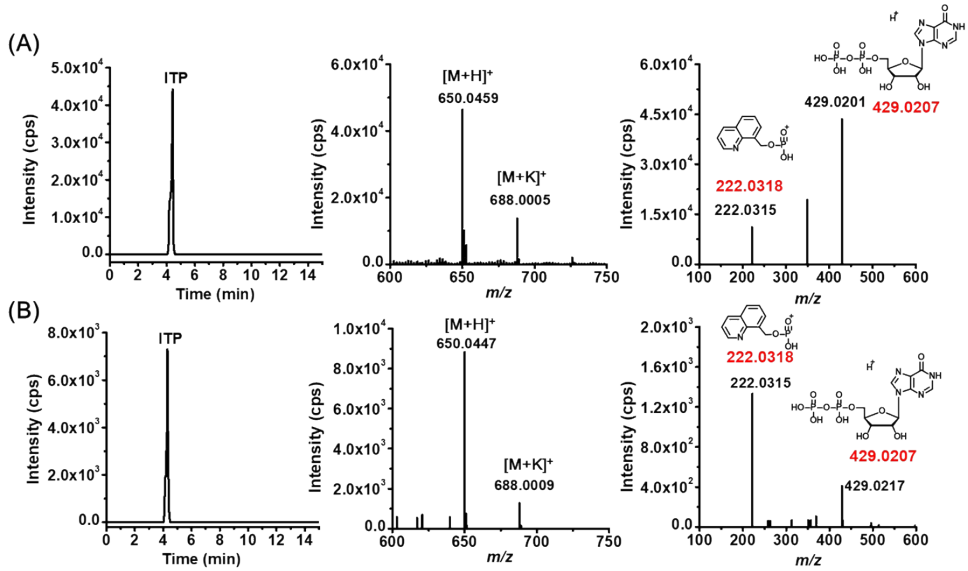

12. XTP

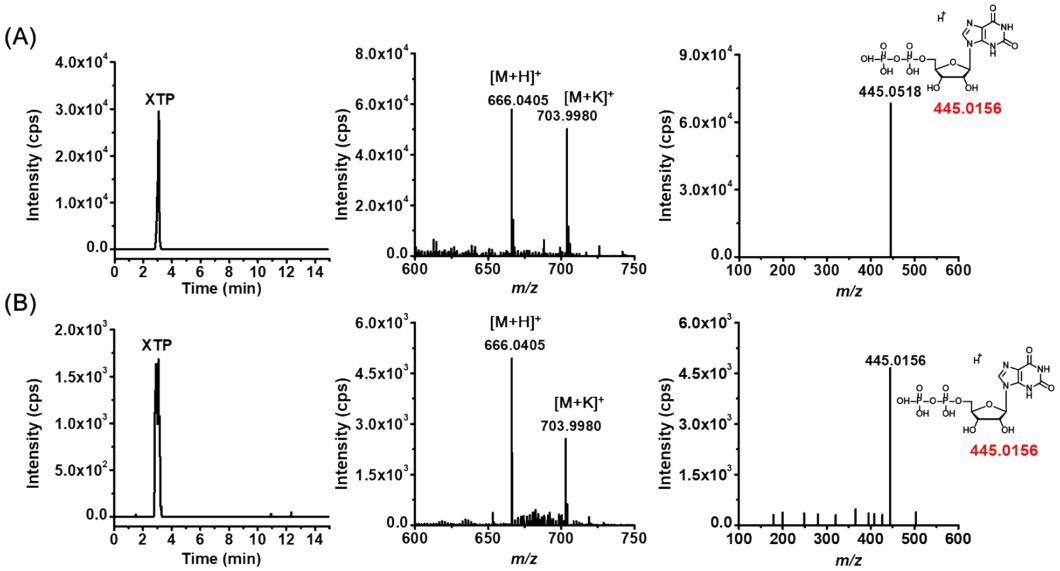

13. N^1-meATP

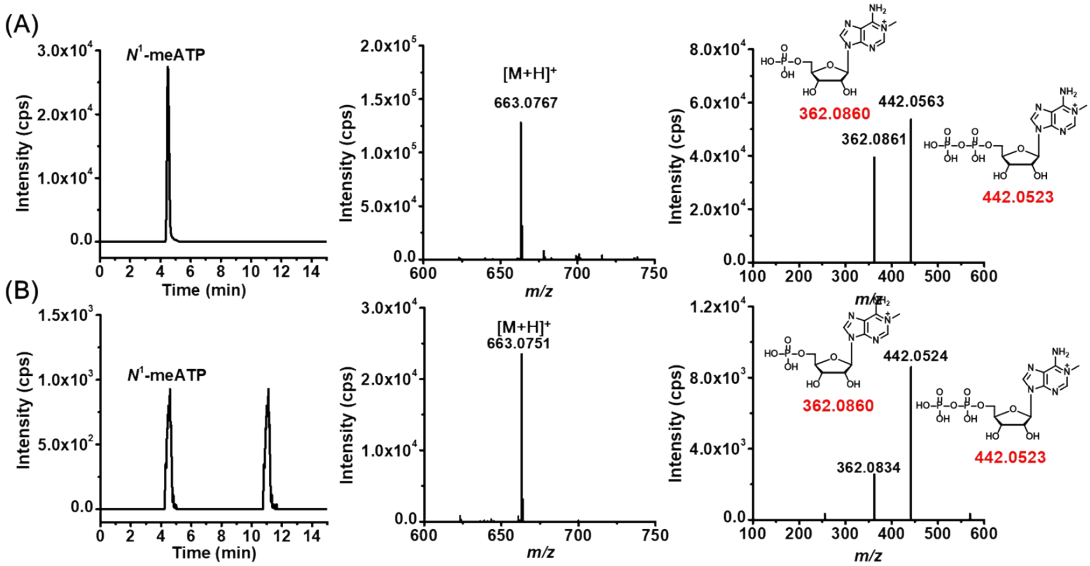

14. 2-S-UTP

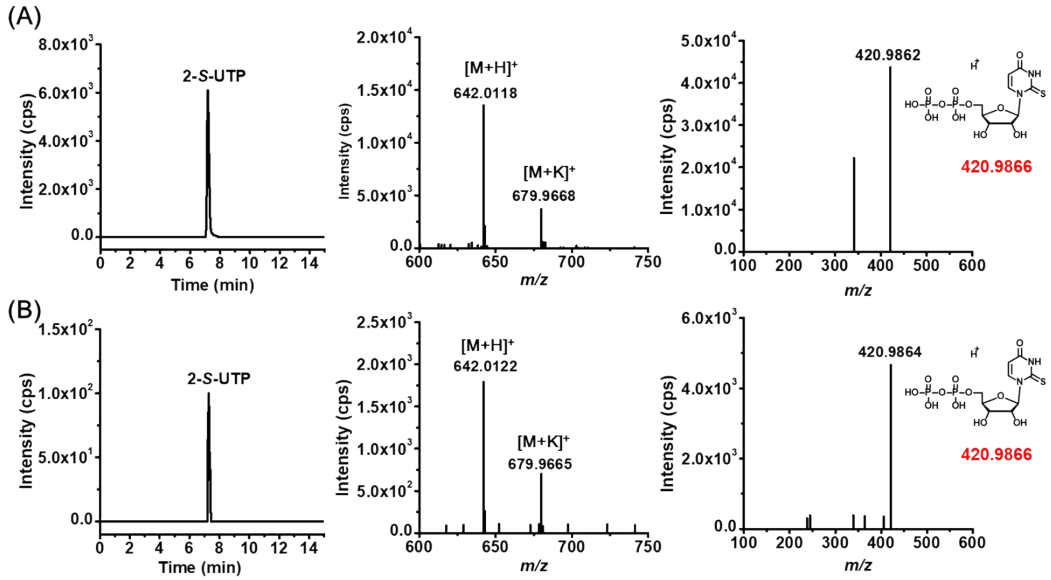

15. 5-hmCTP

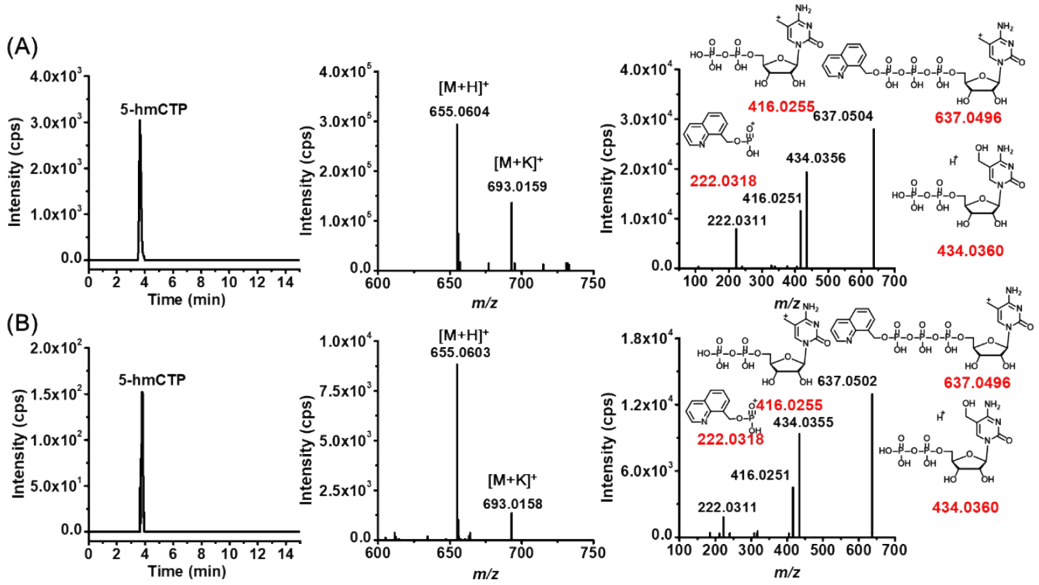

16. 5-hmdCTP

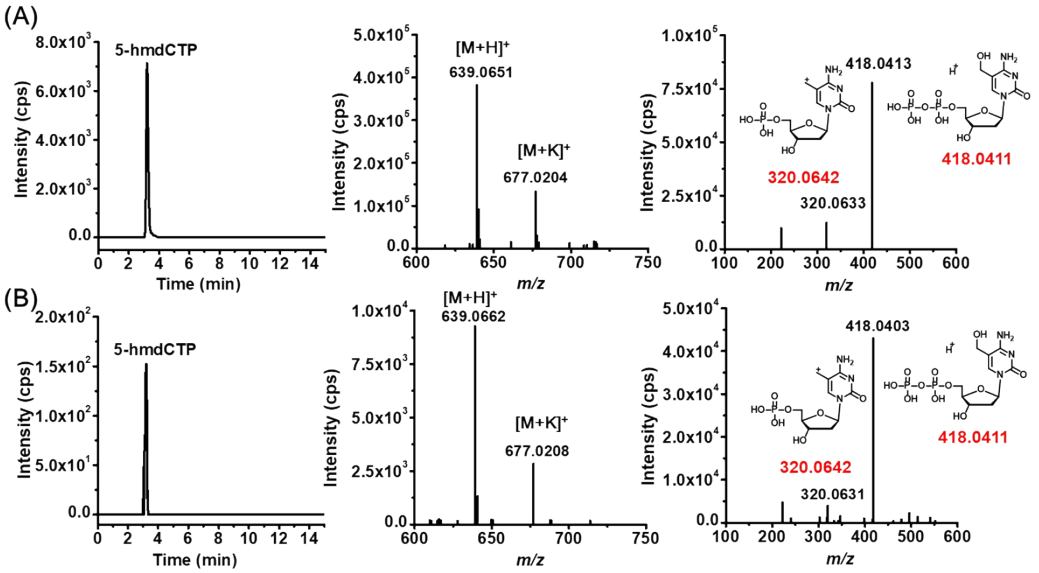

17. 2'-*O*-meATP

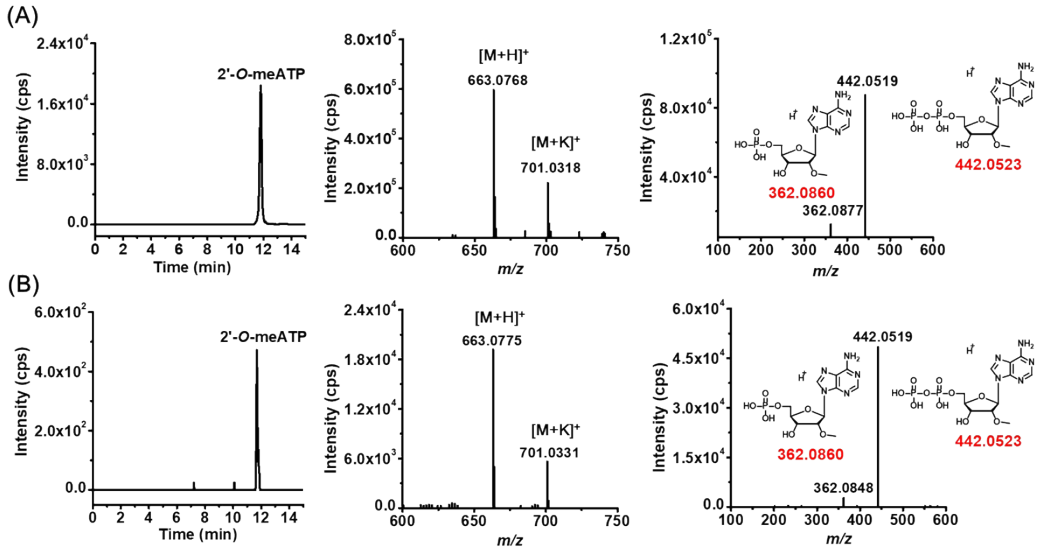

18. 2'-*O*-meGTP

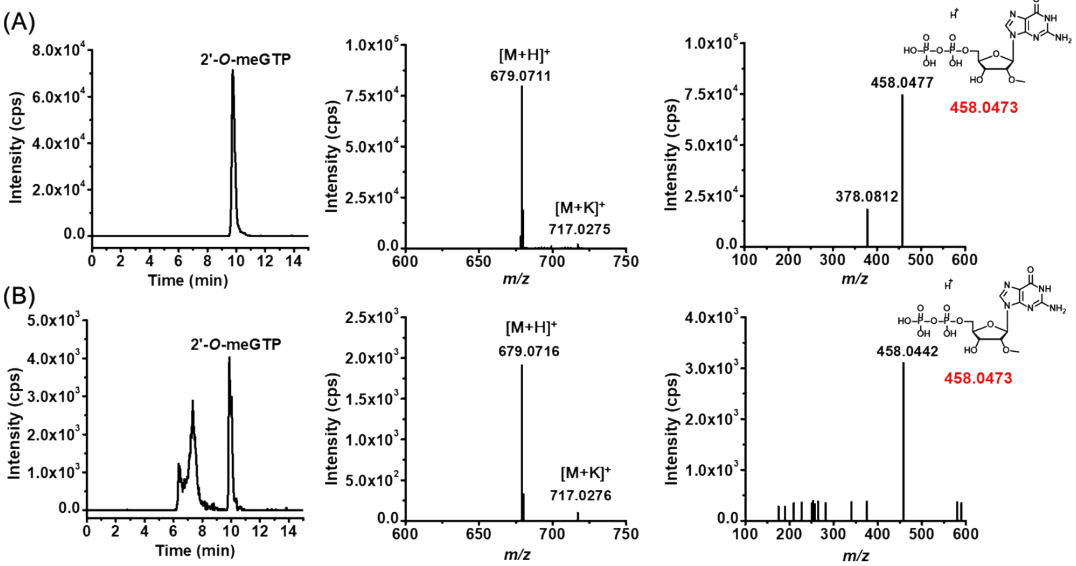
(A)
2'-O-meGTP
Intensity (cps)
Time (min)
[M+H]+
679.0711
[M+K]+
717.0275
m/z
458.0477
458.0473
378.0812
(B)
2'-O-meGTP
Intensity (cps)
Time (min)
[M+H]+
679.0716
[M+K]+
717.0276
m/z
458.0442
458.0473

Figure S11. Schematic illustration of the stable isotope tracing monitored by mass spectrometry. Cells were maintained in L-methionine-free DMEM-KO medium with added D_3-Met. D_3-Met can be converted into CD_3-*S*-adenosyl-L-methionine (SAM), which serves as the methyl donor for DNA and RNA methylation. Therefore, the methyl groups of methylated nucleosides in DNA and RNA carry CD_3. The detectable endogenous methylated NTPs carrying CD_3 indicates that they derive from the degradation of nucleic acids.

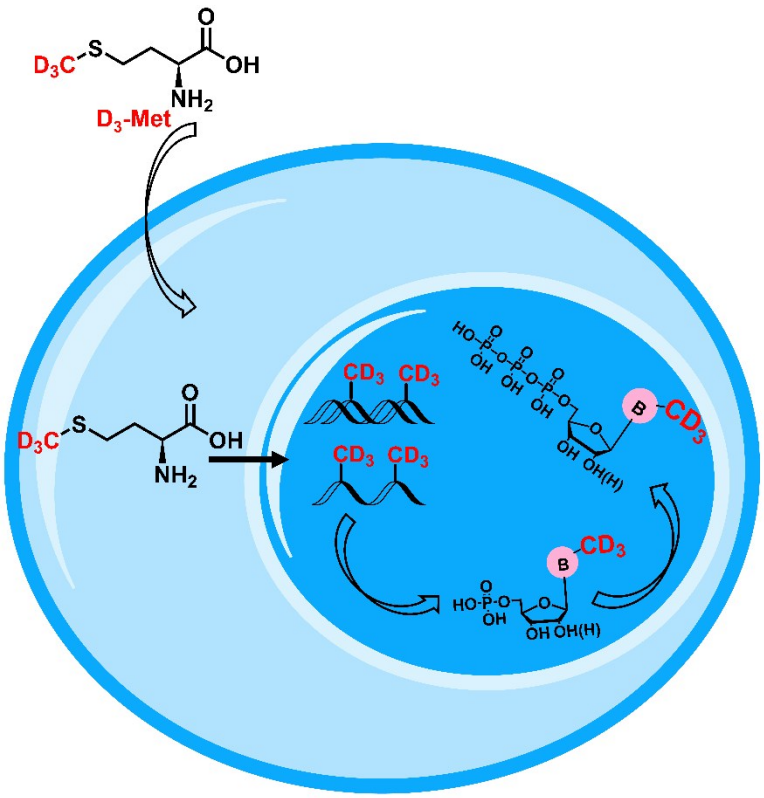

Figure S12. Evaluation of the stable isotope labeling efficiency by using D_3-Met cultured 293T cells. (A) Extracted ion chromatograms of m^1A, Am, m^6A, CD_3-m^1A, CD_3-Am and CD_3-m^6A after D_3-Met labeling. (B) Extracted ion chromatograms of m^7G, Gm, CD_3-m^7G and CD_3-Gm after D_3-Met labeling from RNA. (C) Extracted ion chromatograms of 5-mC and CD_3-5-mC after D_3-Met labeling. (D) Extracted ion chromatograms of 5-mdC and CD_3-5-mdC after D_3-Met labeling. (F) The stable isotope labeling efficiencies by D_3-Met labeling. The stable isotope labeling efficiencies were calculated by comparing the contents of the CD_3-nucleosides with total CD_3- and CH_3 nucleosides (Labeling ratio = CD_3-nucleoside/(CD_3-nucleoside + CH_3-nucleoside)).

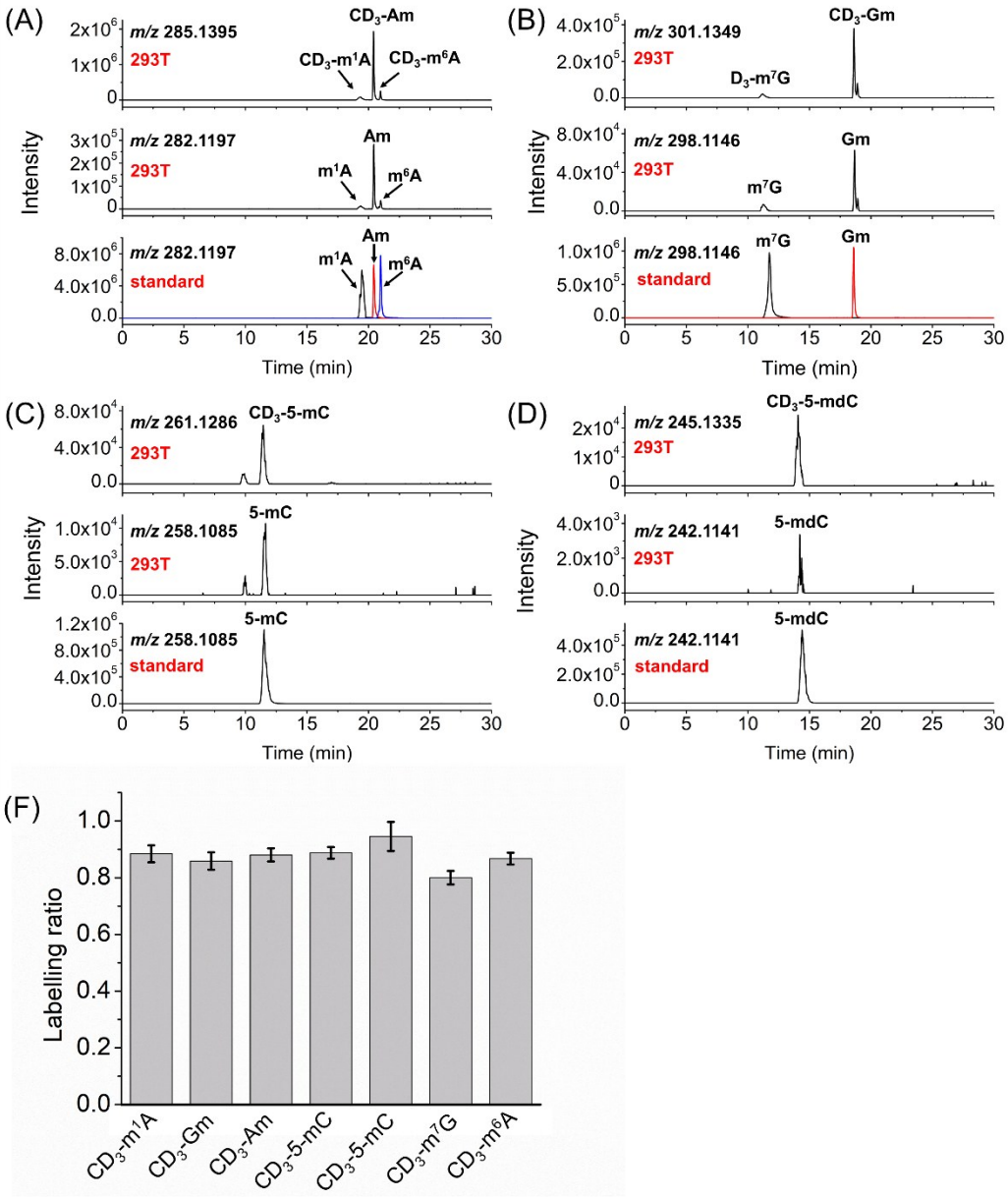

Figure S13. Identification of modified NMPs and NDPs in 293T cells. (A) The extracted ion chromatograms (left panel), high-resolution MS spectra (middle panel) and product ions spectra (right panel) of standards. (B) The extracted ion chromatograms (left panel), high-resolution MS spectra (middle panel) and product ions spectra (right panel) of the compounds detected in 293T cells.

1. ADP

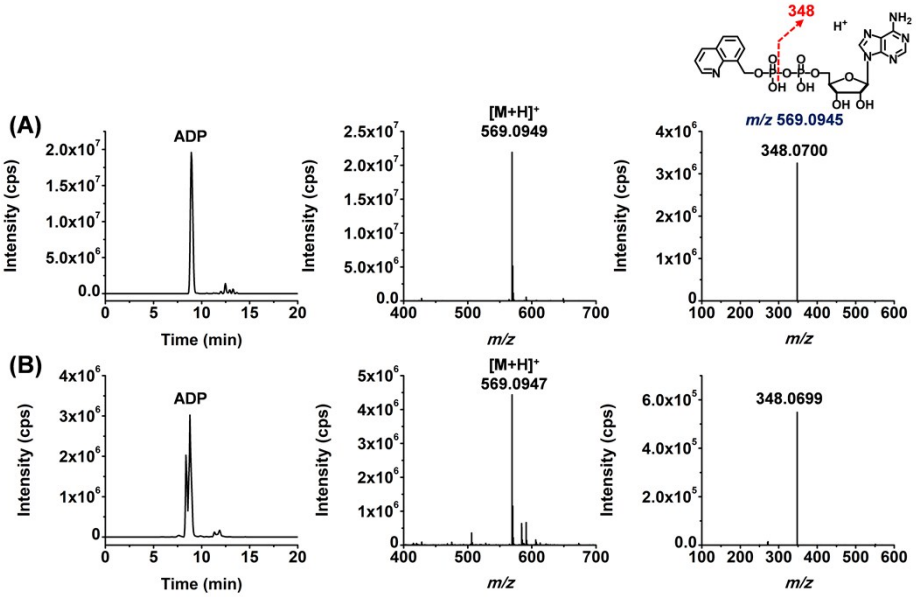

2. AMP

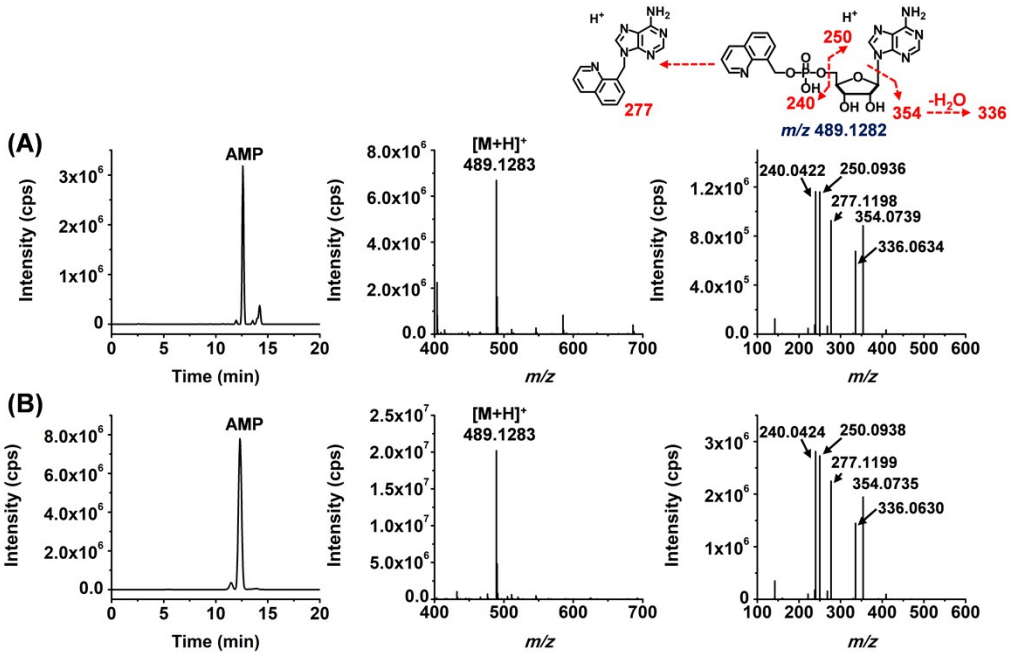

3. dADP

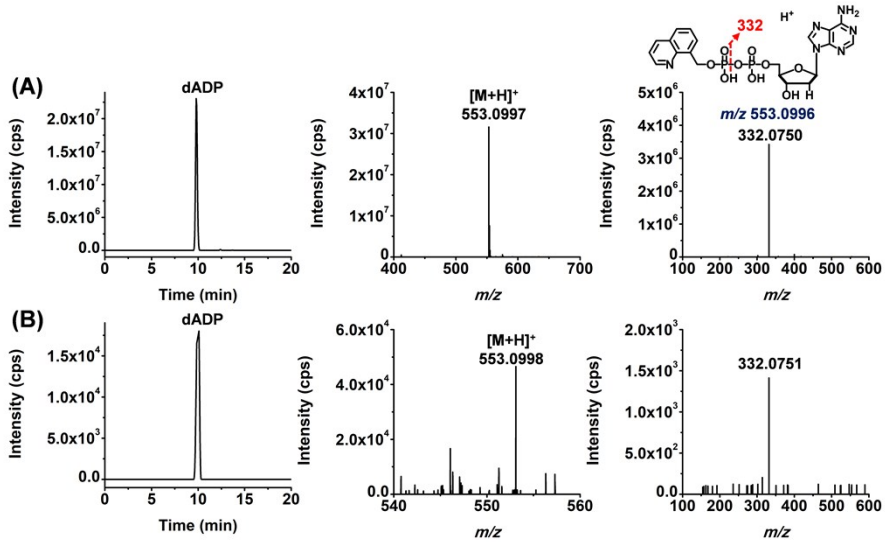

4. dAMP

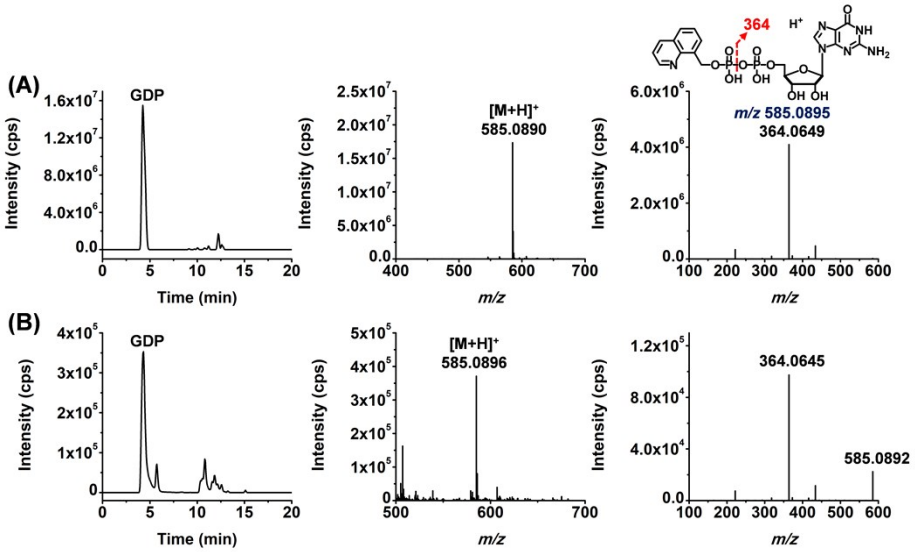

5. GDP

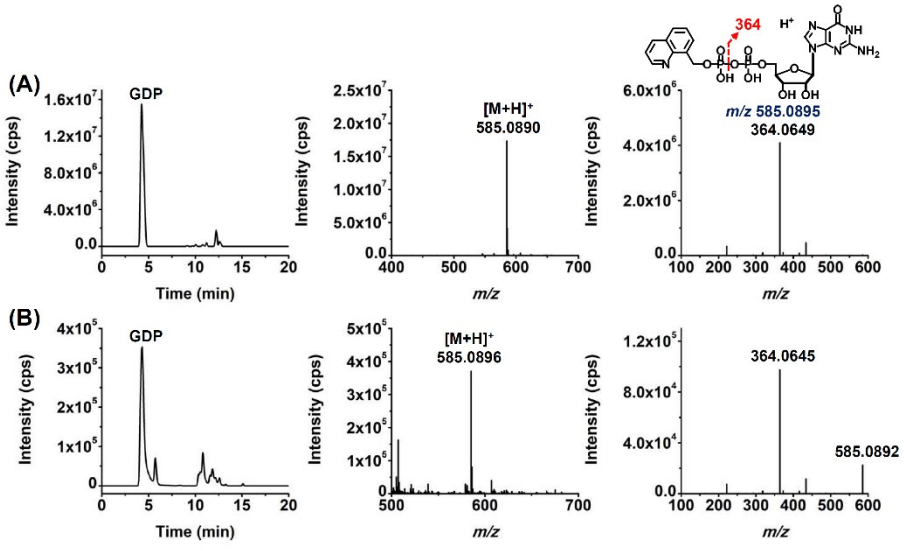

6. GMP

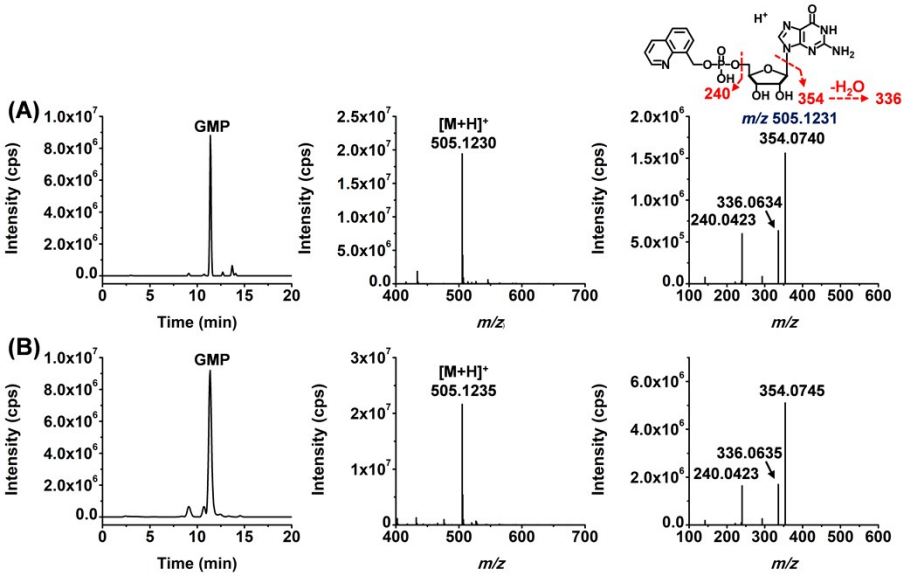

7. dGDP

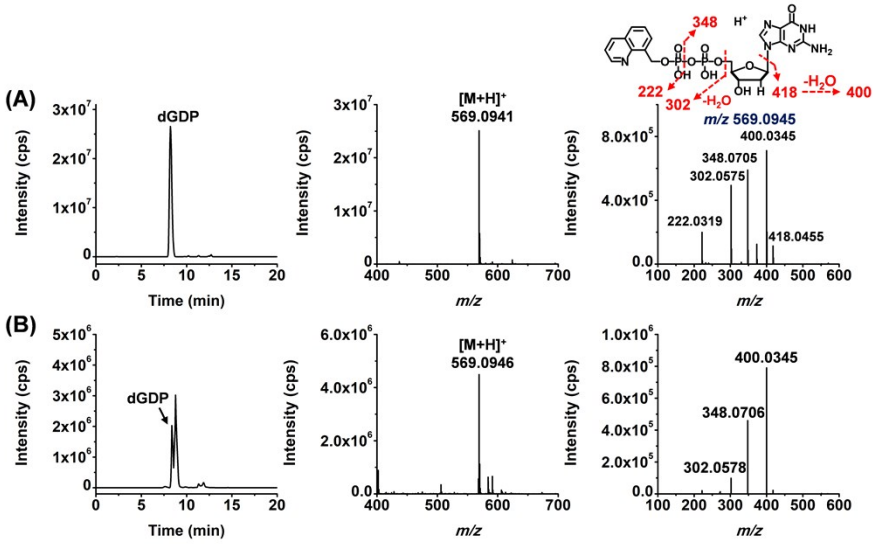

8. dGMP

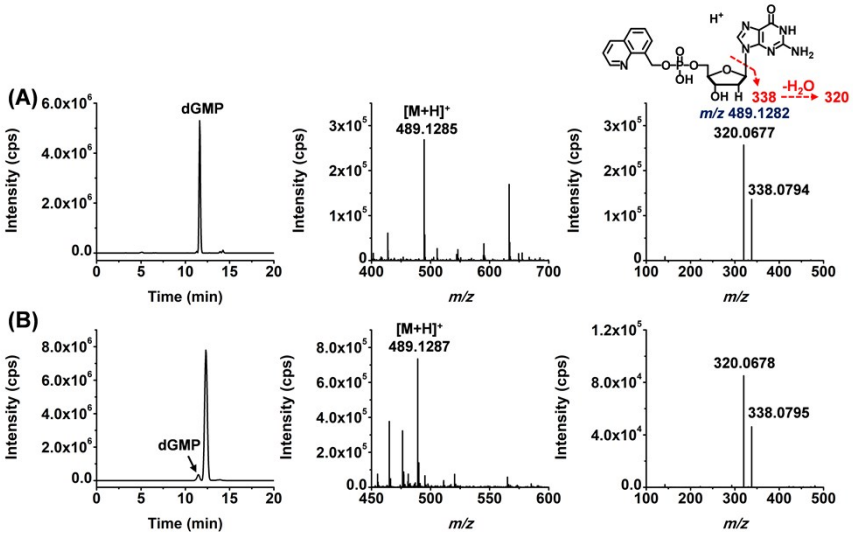

9. CDP

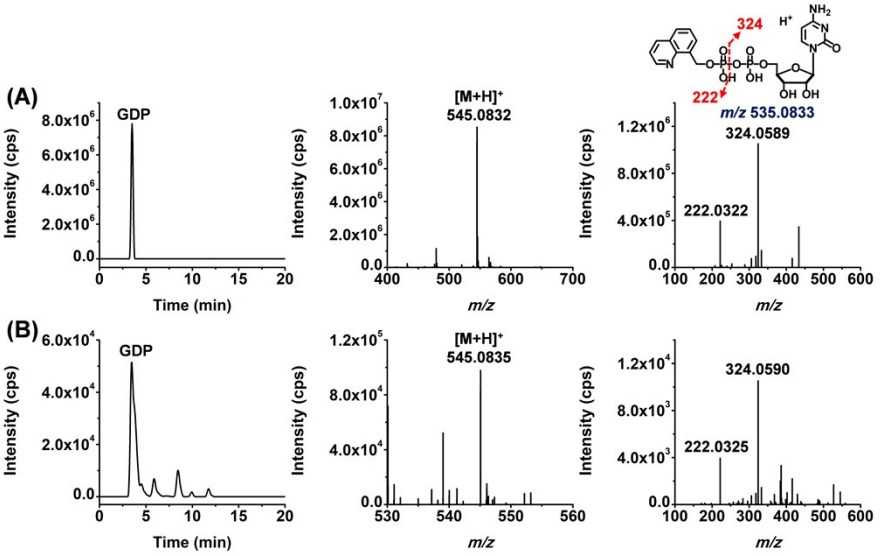

10. CMP

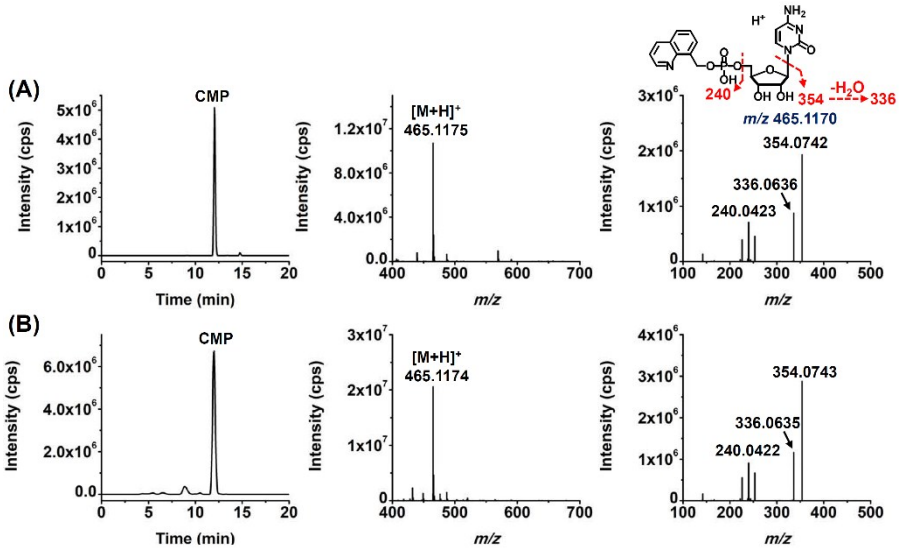

11. dCDP

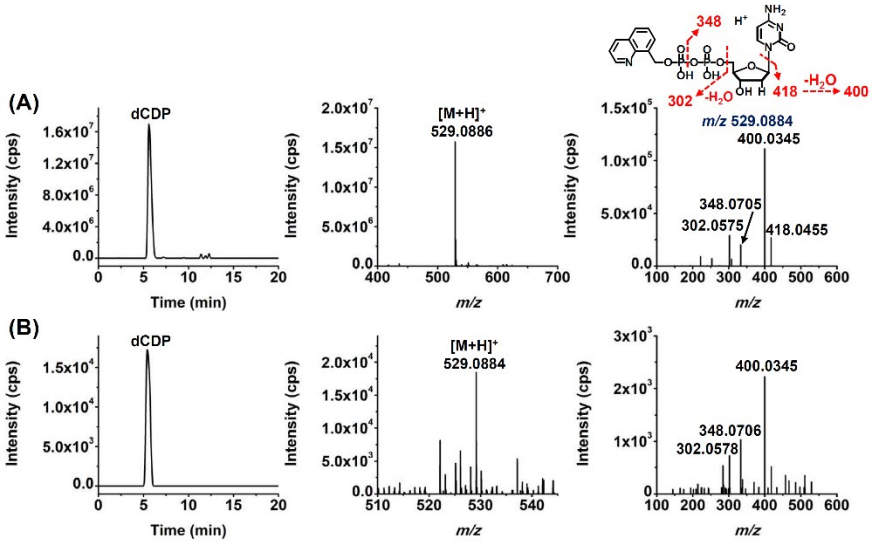

12. dCMP

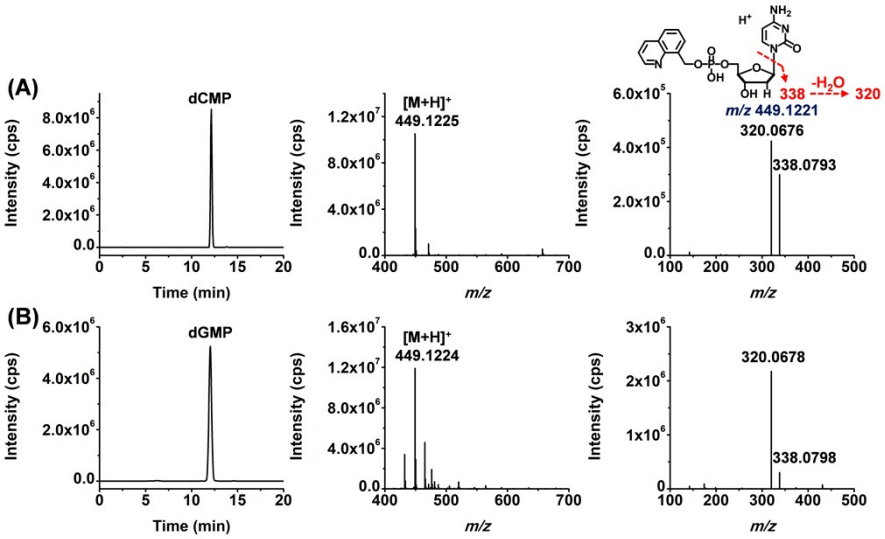

13. UDP

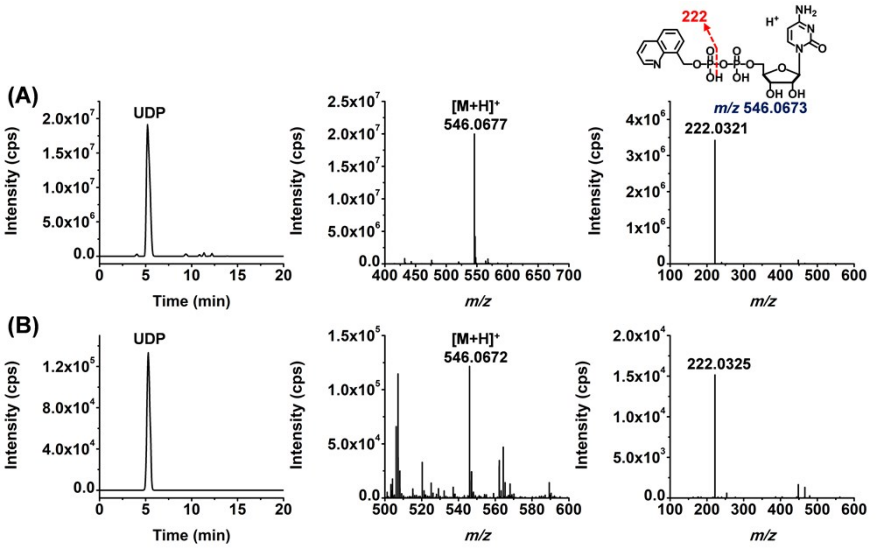

14. UMP

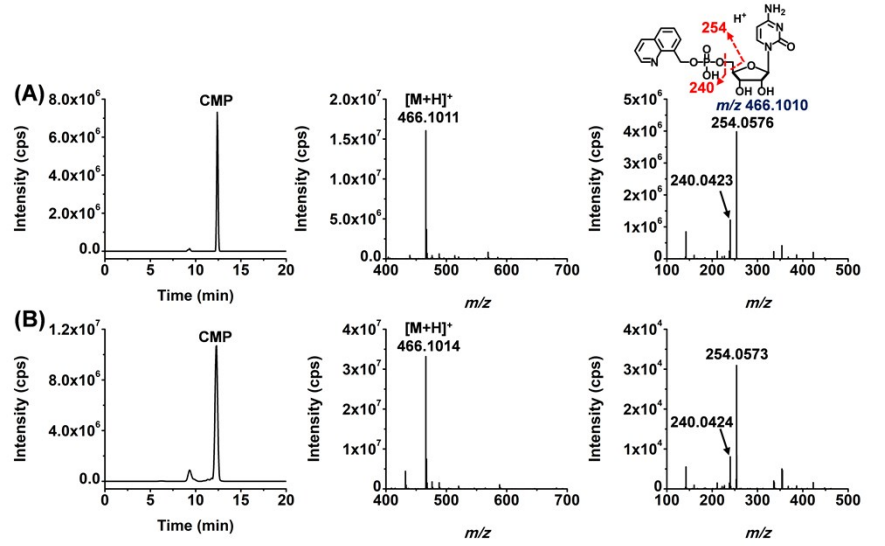

15. TDP

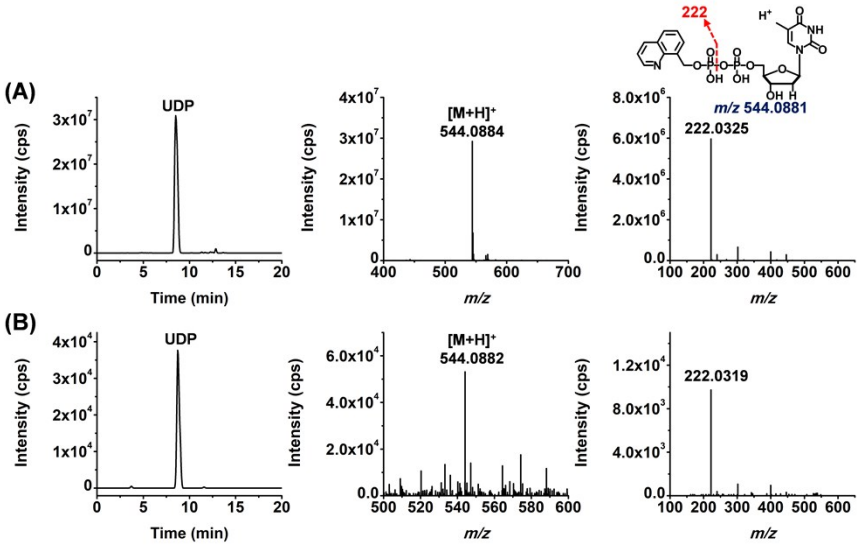

16. TMP

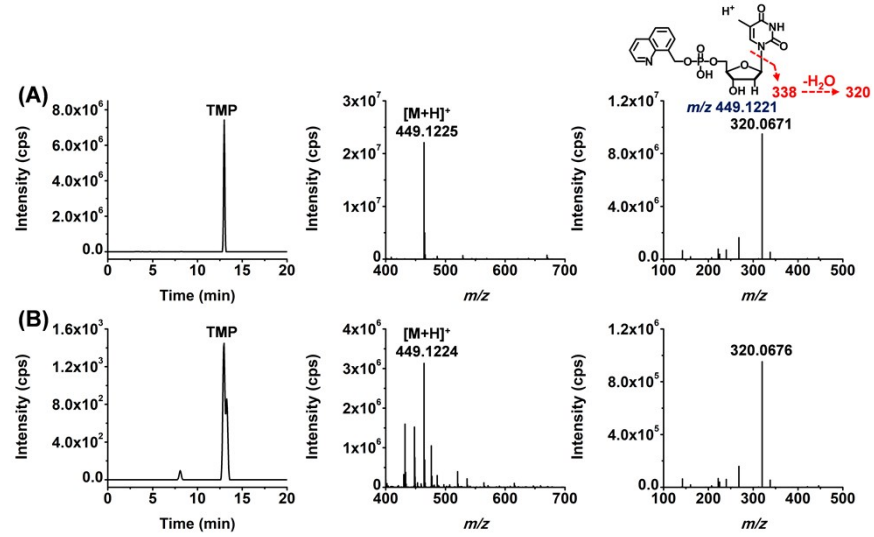

17. N^6-meADP

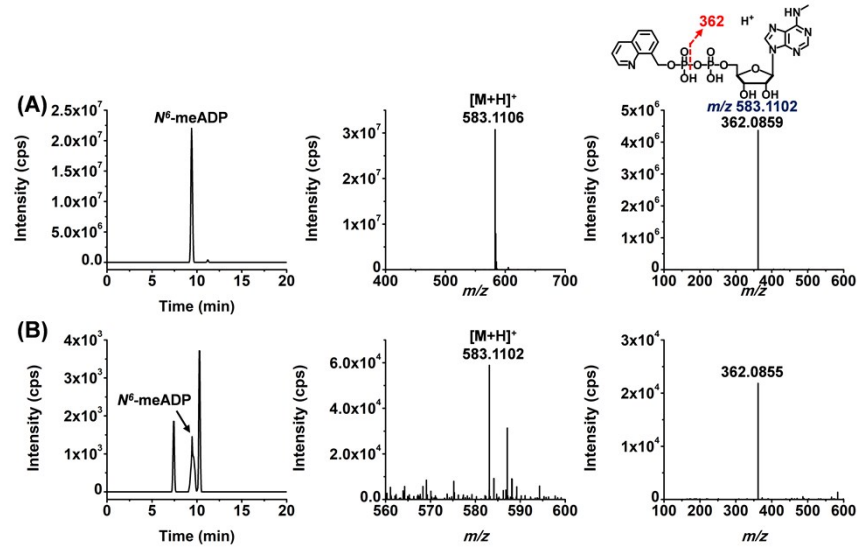

18. N^6-meAMP

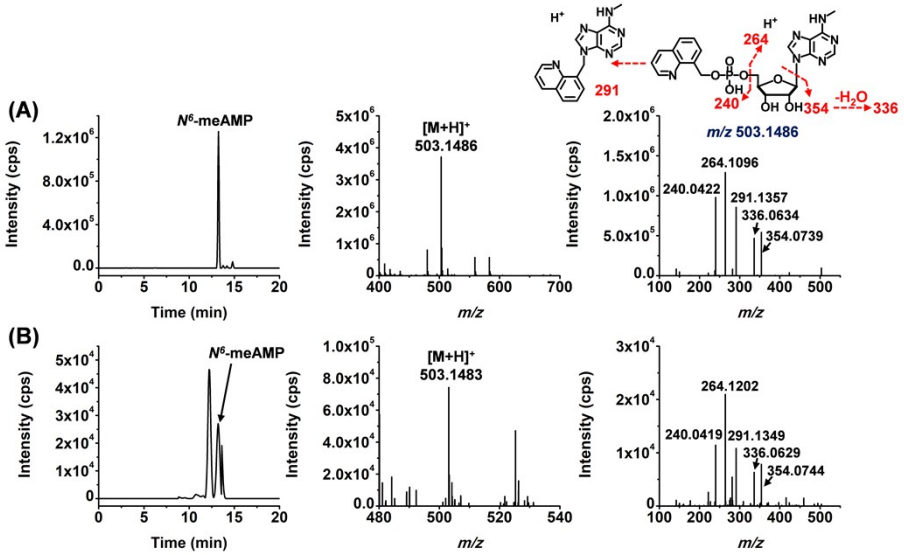

19. 7-meGDP

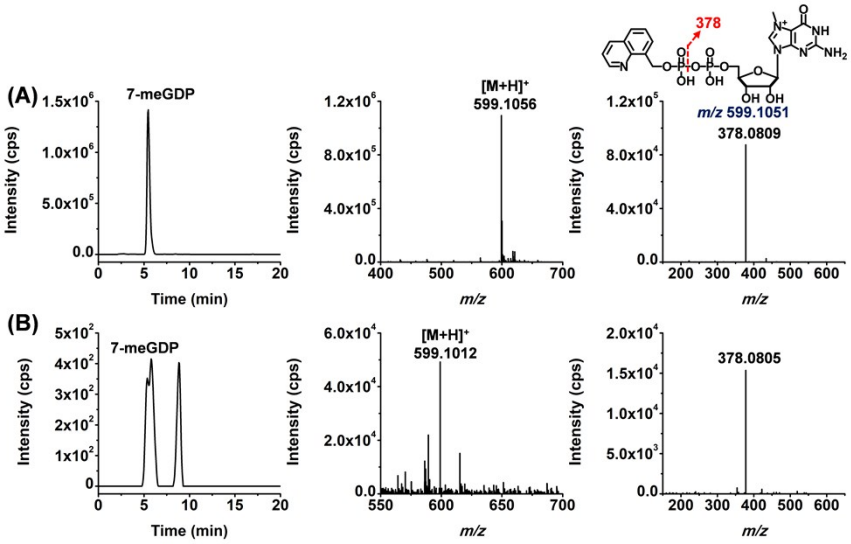

20. 7-meGMP

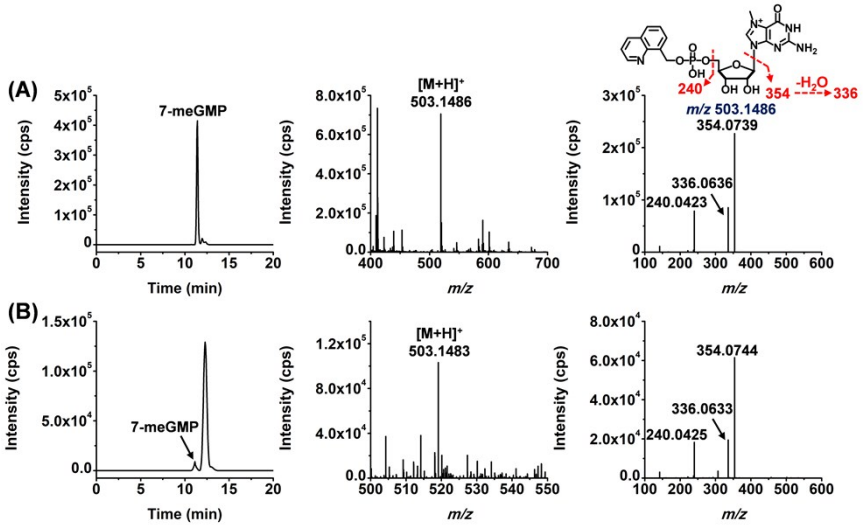

21. IDP

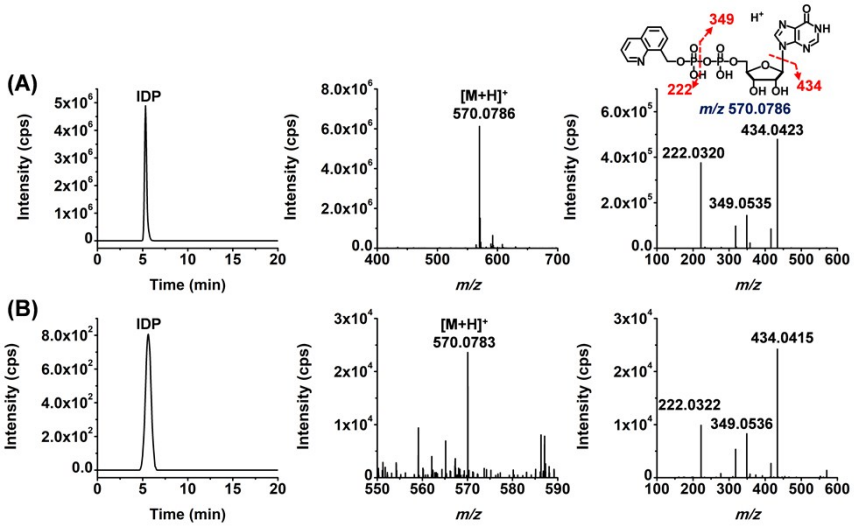

22. IMP

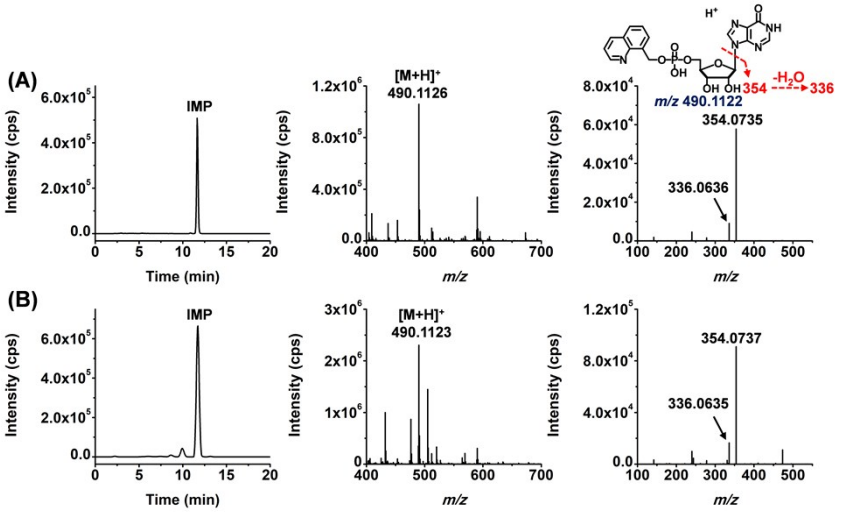

23. XDP

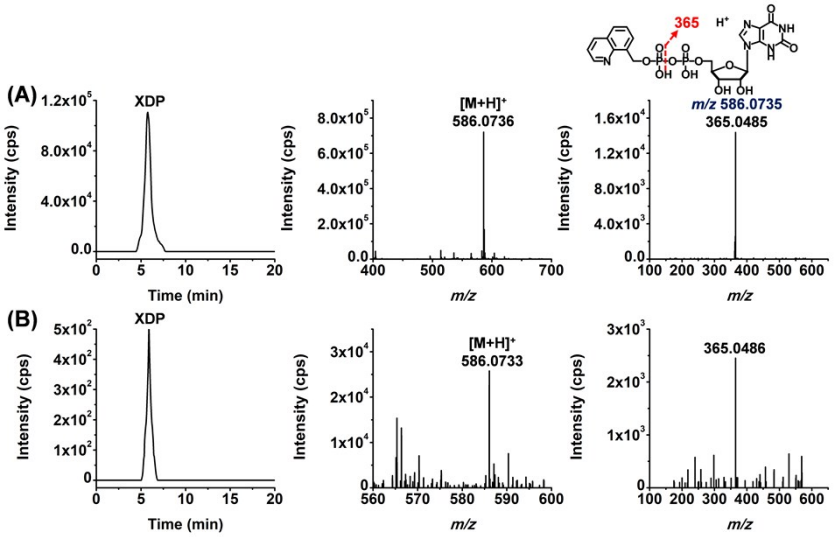

24. XMP

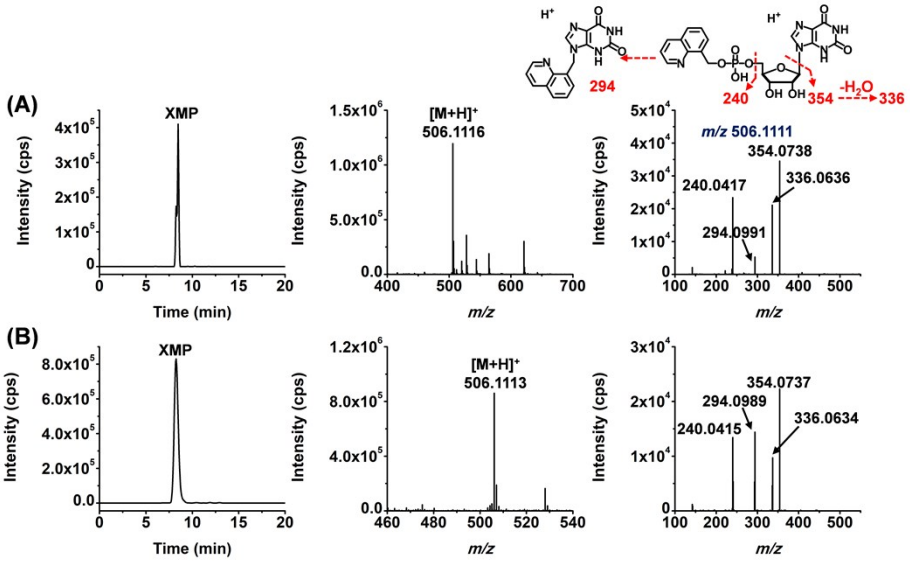

25. N^1-meADP

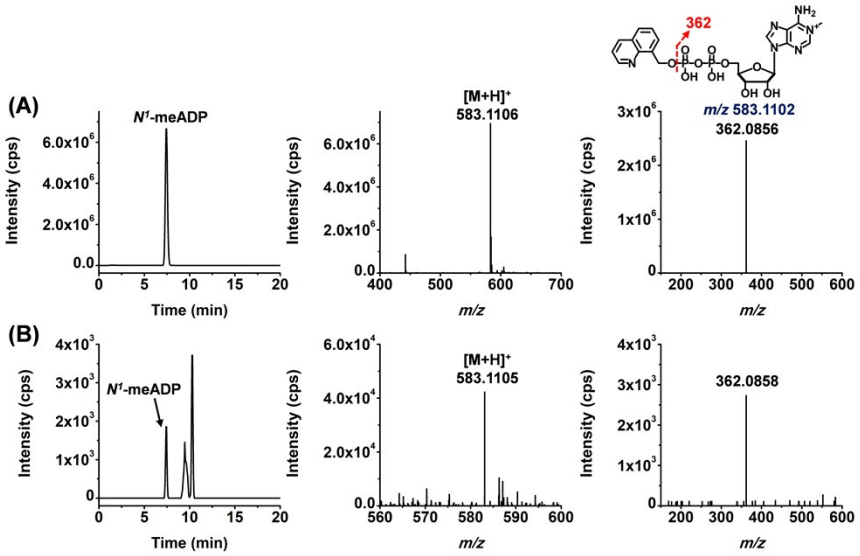

26. N^1-meAMP

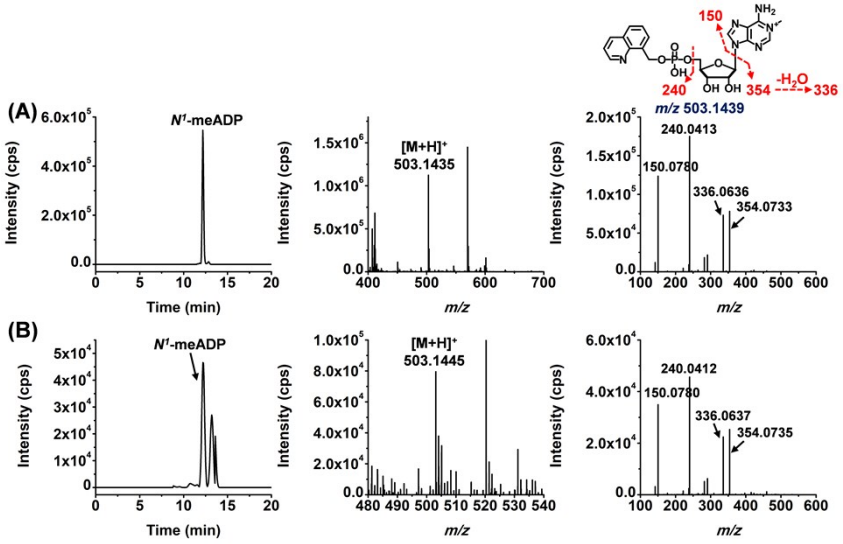

27. 2-S-UDP

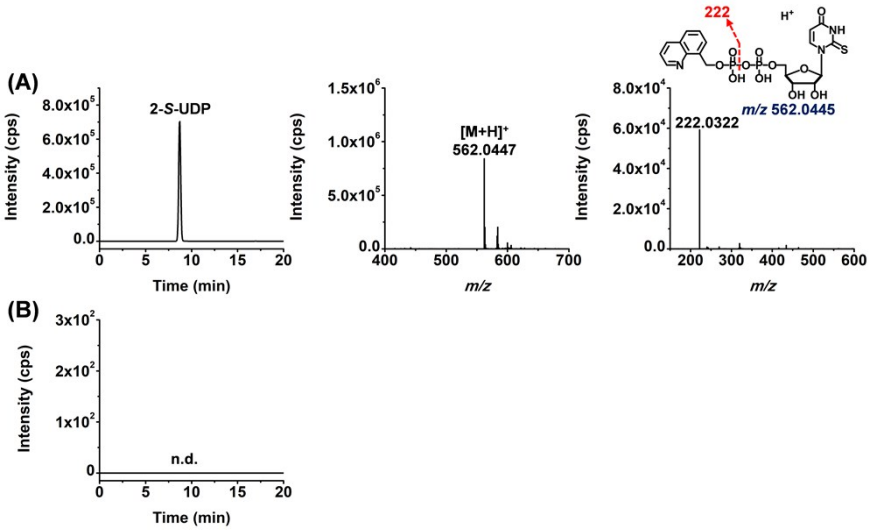

28. 2-S-UMP

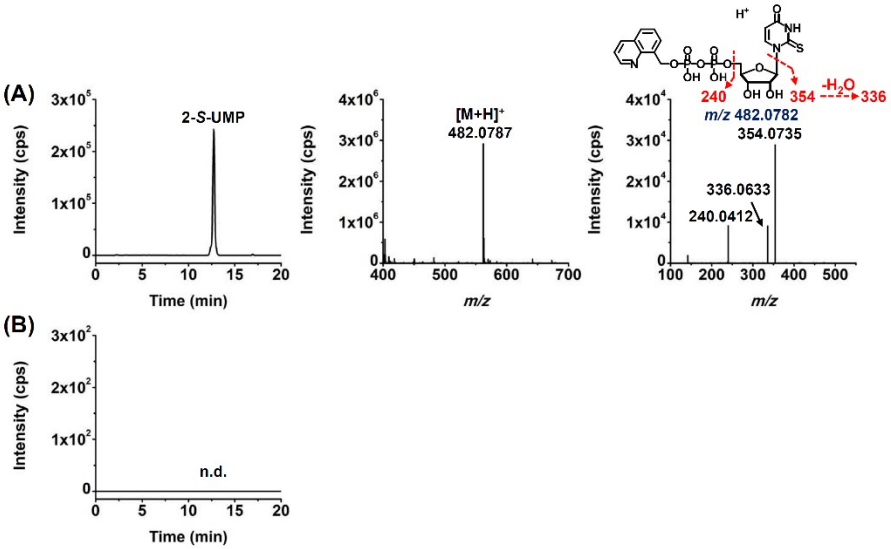

29. 5-meCDP

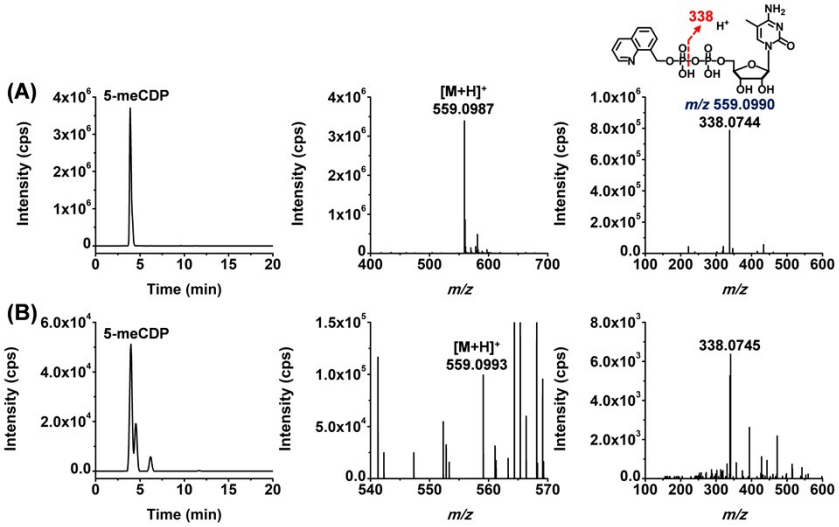

30. 5-meCMP

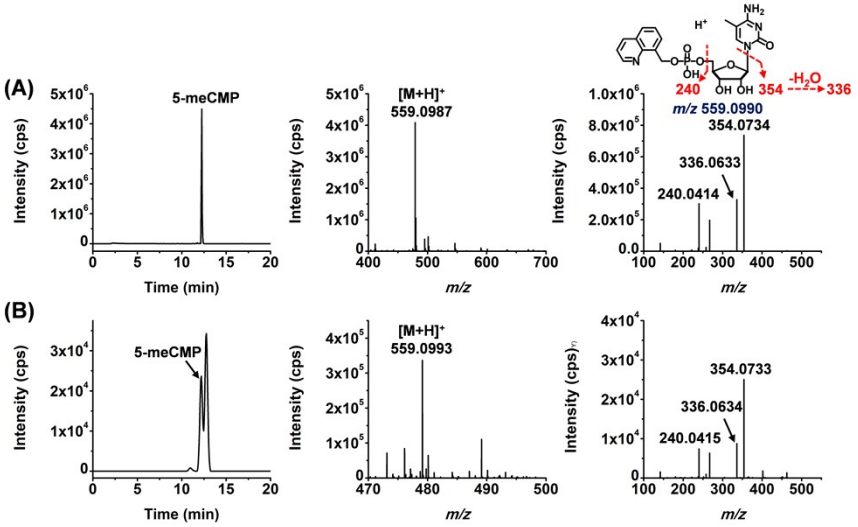

31. 5-medCDP

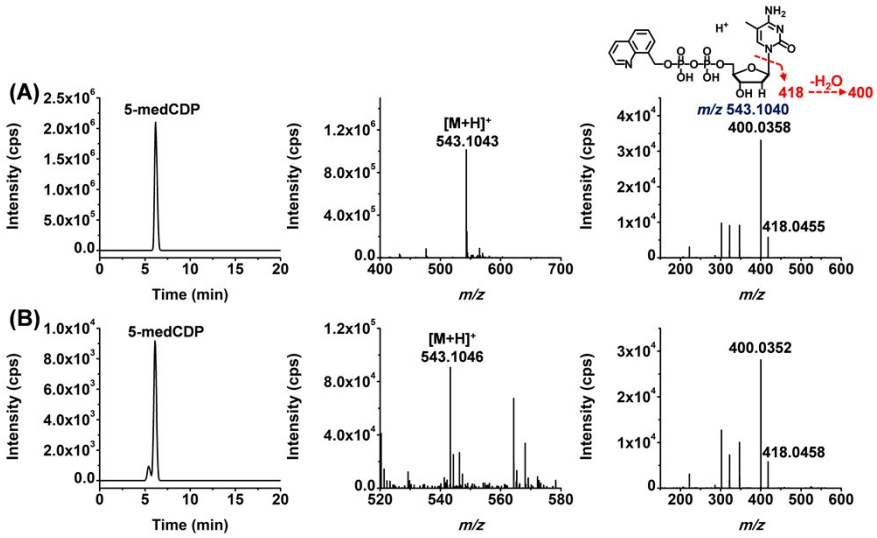

32. 5-medCMP

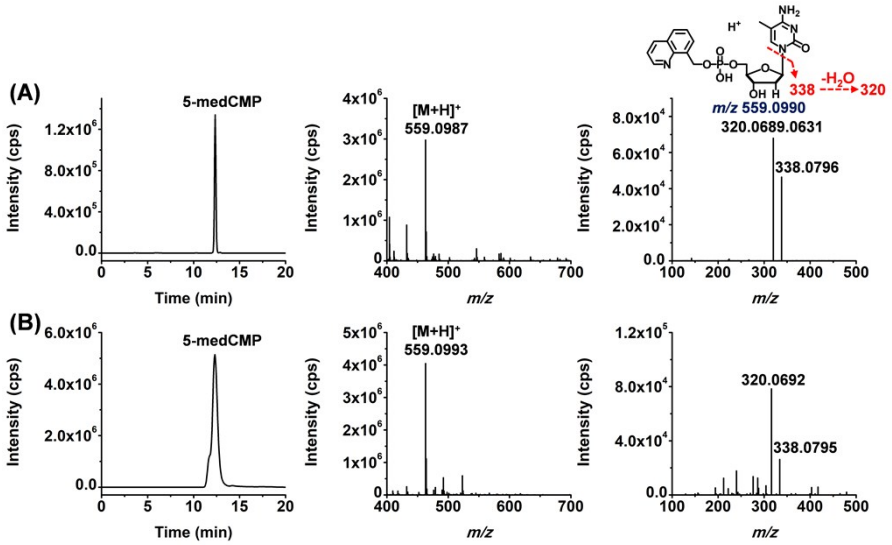

33. 5-hmCDP

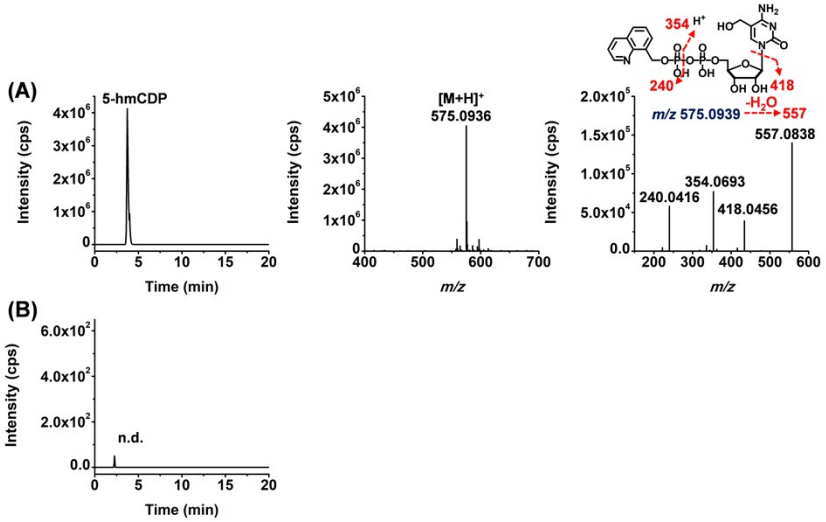

34. 5-hmCMP

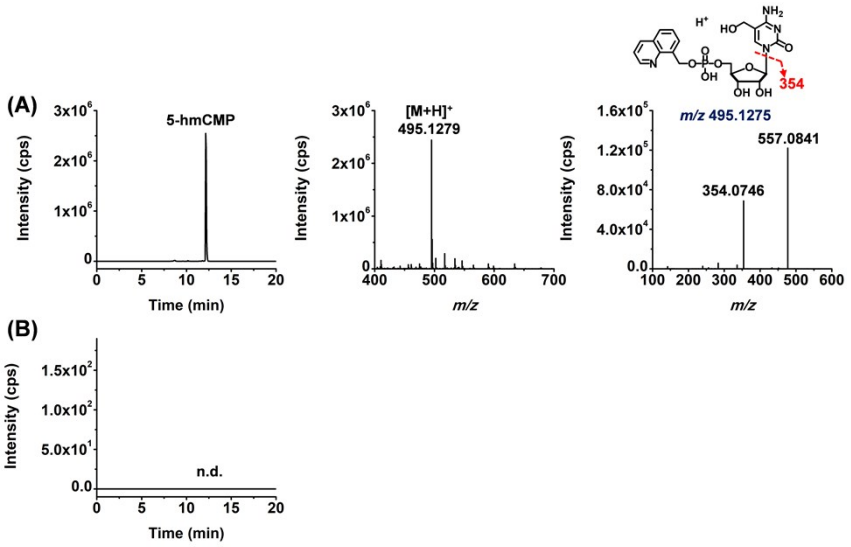

35. 5-hmdCDP

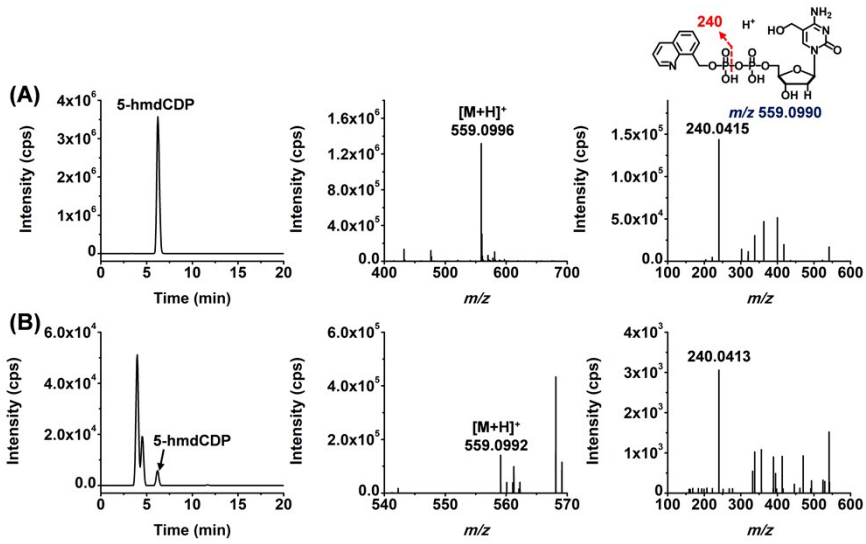

36. 5-hmdCMP

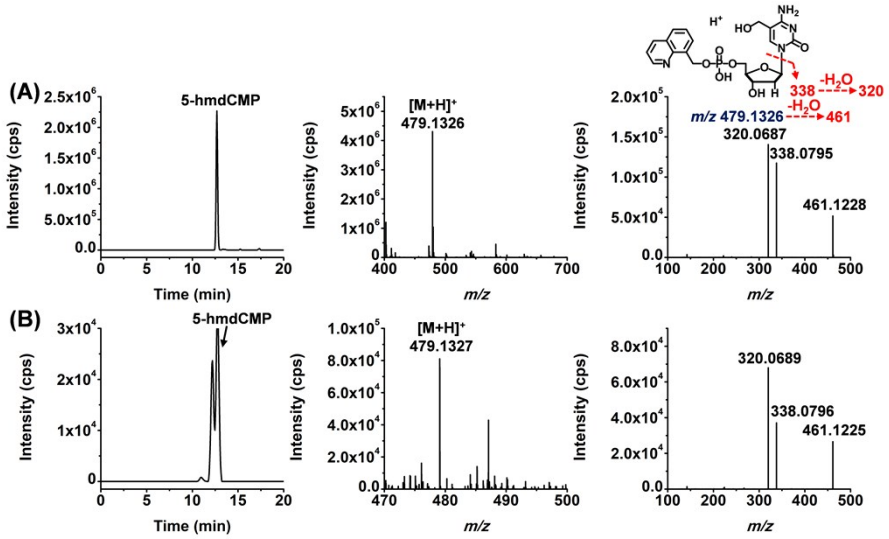

37. 2'-*O*-meADP

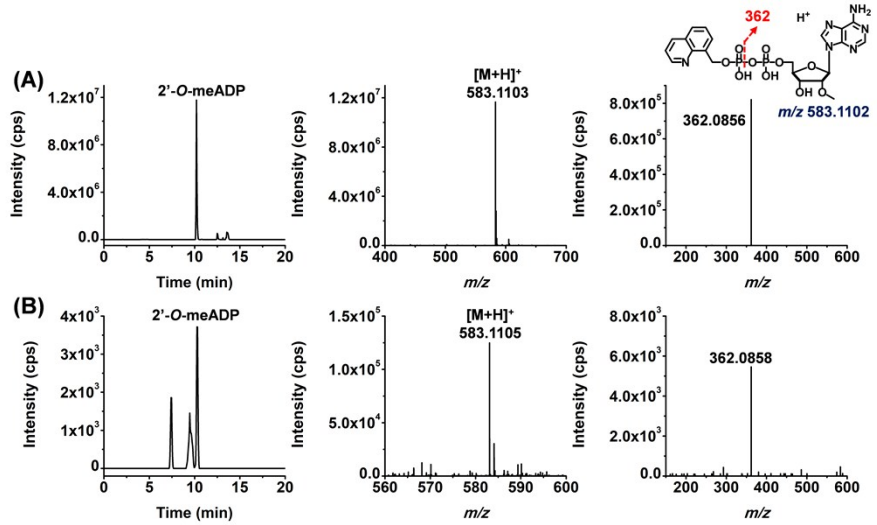

38. 2'-*O*-meAMP

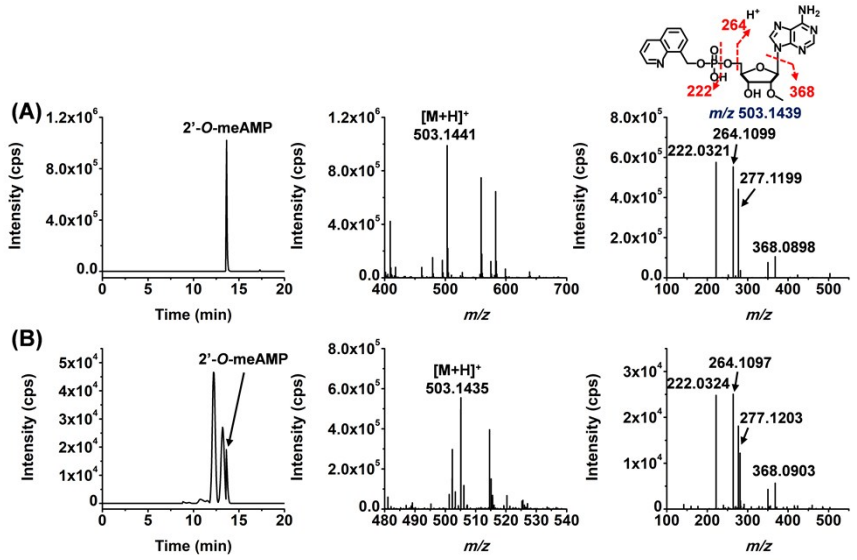

39. 2’-*O*-meGDP

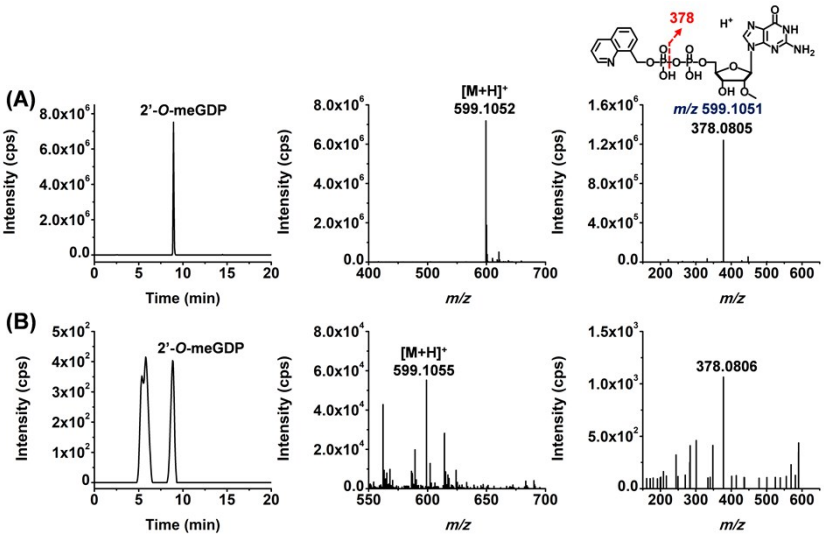

40. 2’-*O*-meGMP

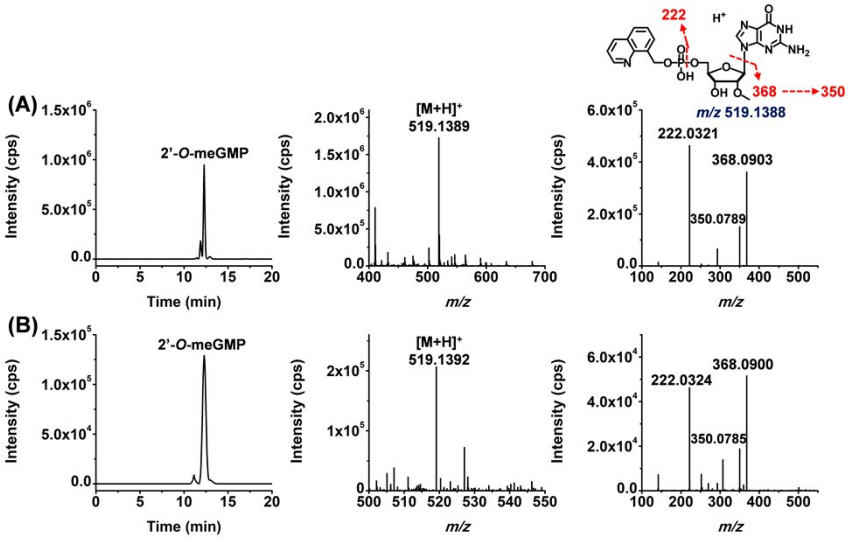

Reference

1. M. Uhrova, Z. Deyl and M. Suchanek, *J Chromatogr B*, 1996, 681, 99-105.
2. M. L. Tassotto and C. K. Mathews, *J Biol Chem*, 2002, 277, 15807-15812.
3. H. T. Feng, N. Wong, S. Wee and M. M. Lee, *J Chromatogr B*, 2008, 870, 131-134.
4. R. M. Seifar, C. Ras, J. C. van Dam, W. M. van Gulik, J. J. Heijnen and W. A. van Winden, *Anal Biochem*, 2009, 388, 213-219.
5. N. Yamaoka, Y. Kudo, K. Inazawa, S. Inagawa, M. Yasuda, K.-i. Mawatari, K. Nakagomi and K. Kaneko, *J Chromatogr B*, 2010, 878, 2054-2060.
6. O. Magdenoska, J. Martinussen, J. Thykaer and K. F. Nielsen, *Anal Biochem*, 2013, 440, 166-177.
7. L. Wu, L. Chen, J. N. Selvaraj, Y. Wei, Y. Wang, Y. Li, J. Zhao and X. Xue, *Food Chem*, 2015, 173, 1111-1118.
8. M. Ishimaru, M. Haraoka, H. Hatate and R. Tanaka, *Food Anal Methods*, 2016, 9, 1606-1615.
9. J. Y. Puy, L. P. Jordheim, E. Cros-Perrial, C. Dumontet, S. Peyrottes and I. Lefebvre-Tournier, *J Chromatogr B*, 2017, 1053, 101-110.
10. P. Fedorov, R. Grabic, G. Fedorova, J. Cosson, S. Boryshpolets and B. Dzyuba, *Czech J Anim Sci*, 2017, 62, 67-74.